LOAD-ABSORPTION AND INTERACTION OF TWO FILAMENTS IN A FIBER-REINFORCED MATERIAL

Thesis by

Thomas Glen Carne

In Partial Fulfillment of the Requirements

for the Degree of

Doctor of Philosophy

California Institute of Technology

Pasadena, California

1973

(Submitted September 20, 1972)

To my parents

in appreciation for all that

they have done for me.

Acknowledgments

The author wishes to express his deepest appreciation to Professor James K. Knowles for his guidance during this investigation and his substantial aid in the preparation of this thesis. The assistance and suggestions of Professor Eli Sternberg and Professor Rokuro Muki are also appreciated.

Special thanks are due to Mrs. Julie Powell for her truly expert typing of this manuscript and her endless patience. The author also wishes to thank his wife Joyce for all of her help and encouragement.

The financial support received from the National Science Foundation and the Office of Naval Research is gratefully acknowledged.

Abstract

This investigation is concerned with the interaction — as far as load-absorption is concerned — of a pair of identical and parallel elastic filaments in a fiber-reinforced composite material. The filaments are assumed to have uniform circular cross-sections, are taken to be semi-infinite, and are supposed to be continuously bonded to an all-around infinite matrix of distinct elastic properties. At infinity the matrix is subjected to uniaxial tension parallel to the filaments. Two separate but related problems are treated. In the first both filaments extend to infinity in the same direction and their terminal cross-sections are coplanar. In the second problem the filaments extend to infinity in opposite directions and their terminal cross-sections need no longer be coplanar, the two filaments being permitted to overlap partly. An approximate scheme based in part on three-dimensional linear elasticity and developed originally by Muki and Sternberg is employed in the analysis. The problems are ultimately reduced to Fredholm integral equations which characterize the distribution of the axial filament force. The integral equations are analyzed asymptotically and numerically. Results are presented which show the variation of filament force with position and the effect on this variation of various relevant geometrical and material properties.

Table of Contents

Introduction.

Fiber-reinforced composite materials have attracted much attention in recent years because their characteristically high strength-to-weight ratios often make them ideal for use as structural components. Among such composites, those reinforced with discontinuous fibers – rather than continuous ones – are of particular interest, since some high-strength fibers can be produced only in relatively short segments. Moreover, short fibers are more adaptable for certain applications such as molding.

In the present investigation we are concerned with the interaction of adjacent filaments in a fiber-reinforced composite, with emphasis on the load-absorption properties of discontinuous filaments. In particular we wish to estimate that separation distance between two parallel filaments at which the interaction effects are negligible insofar as fiber load-absorption is concerned. With this objective in mind we examine analytically two idealized but basic problems in detail. Problem 1 consists of determining the response to uniaxial tension at infinity of a composite comprised of two parallel semi-infinite*, circular cylindrical elastic filaments bonded to an infinite elastic matrix of distinct material properties. The circular end sections of the filaments are coplanar, and both filaments lie on the same side of the plane containing their end sections. The filament

*Discontinuous filaments of practical interest have length-to-diameter ratios which may exceed 1000.

axes are parallel to the applied uniaxial tension. We shall refer to Problem 1 as the twin problem (see Figure 1).

In Problem 2 (the overlap problem) we again consider two parallel semi-infinite circular cylindrical elastic filaments surrounded by an elastic matrix and loaded at infinity by uniaxial tension parallel to the filaments. However, the filament axes now extend to infinity in opposite directions, and the circular ends of the filaments need not lie in the same plane (Figure 2).

In both problems we shall assume perfect bonding between filaments and matrix, and our analysis will be based on the assumption of small deformations in both filaments and matrix. The objective is to determine the variation with position of the axial force within each filament. In particular we shall ascertain the rate at which this force approaches its asymptotic value at infinity, as well as the way in which this rate of approach is effected by the various relevant material and geometrical parameters. The most important parameter for present purposes is the separation distance between the parallel fibers.

The two problems described above possess a useful symmetry which assures that, in each problem, the distribution of axial filament force is identical in the two fibers.

Problems involving load transfer in fiber-reinforced composites in uniaxial tension have been the subject of several previous analytic investigations. Dow [1] in 1963 and Rosen [2] in 1965 examined a single filament of finite length on the basis of a one-dimensional

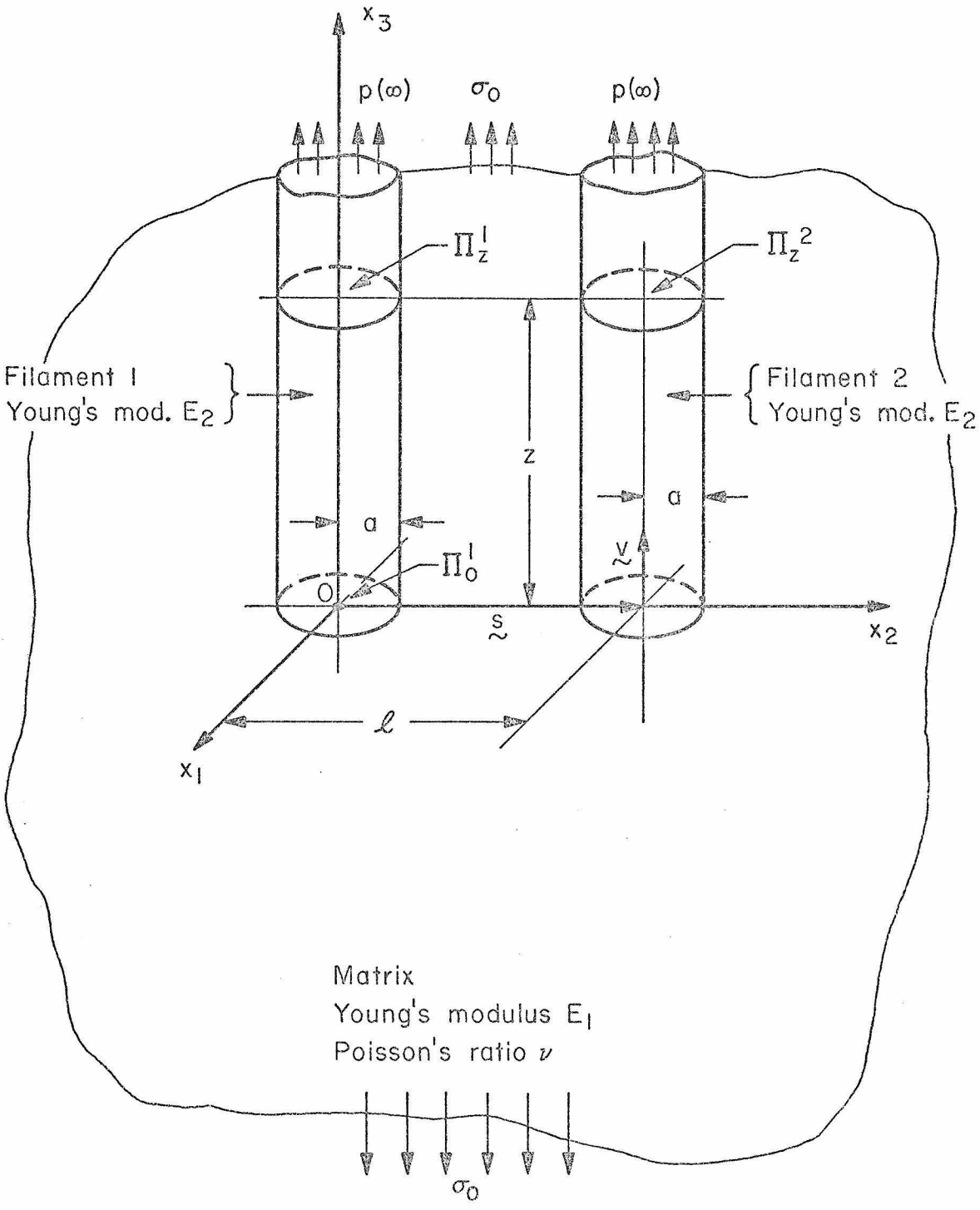

FIGURE 1. TWIN FILAMENTS WITH MATRIX, PROBLEM I

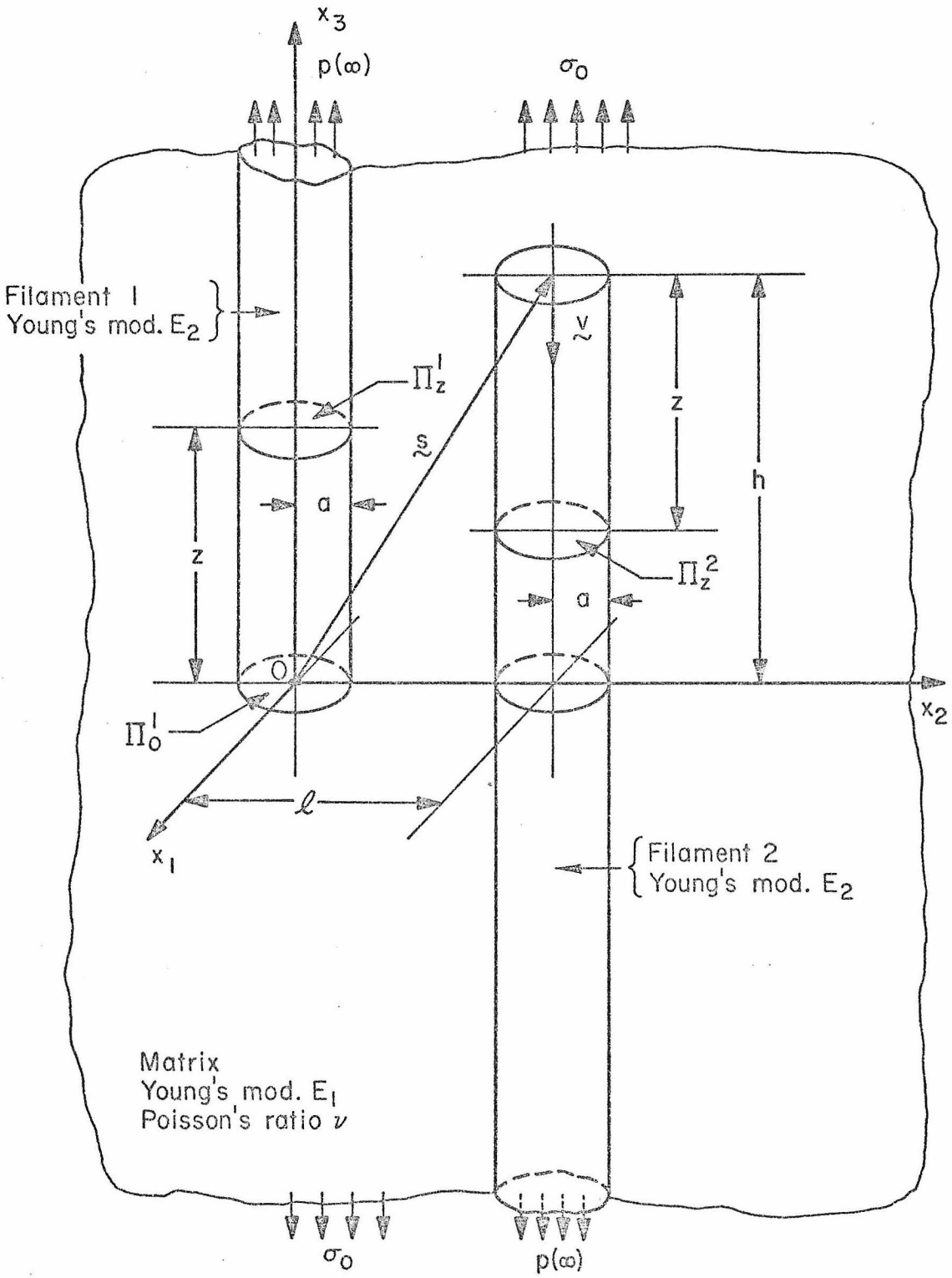

FIGURE 2. OVERLAPPING FILAMENTS WITH MATRIX, PROBLEM 2

treatment of both fiber and matrix. Their results include formulas characterizing the distribution of axial force in the filament.

In 1970 Sternberg and Muki [3] consider a single semi-infinite filament in an elastic matrix with the aid of a more refined model in which the matrix is studied on the basis of three-dimensional linear elasticity, while the fiber is treated as one-dimensional. In an effort to confirm the validity of a model of this type for the single-filament composite, Sternberg and Muki [4] had earlier studied the problem of a doubly-infinite fiber in an infinite matrix subject to a loading uniformly distributed over, and confined to, a single cross-section of the filament. The problem was treated on the basis of two different schemes, in one of which the filament was analyzed one-dimensionally while the matrix was viewed as three-dimensional. In the second scheme, both filament and matrix were examined on the basis of the three-dimensional linear theory of elasticity. The agreement between results obtained in [4] for the axial filament force using the two models was quite favorable and lends substantial credibility to the approach in which the filament is regarded as a one-dimensional elastic continuum, while the matrix is treated three-dimensionally. Such an approach, as developed in [3], forms the basis for the formulation of both problems considered in the present work.

In 1967 Cohen and Romualdi [5] examine the problem of multiple fiber interactions in a composite subject to uniaxial tension. They consider a periodic array of infinitely many parallel, identical filaments and devise an approximate model in which fibers are treated

as one-dimensional, the matrix as three-dimensional. The analysis is entirely numerical.

A finite-element, equivalent-stiffness scheme was used by Chen [6] to investigate a problem of strength in uniaxial tension in a composite containing parallel fibers of finite length. The maximum stress in a fiber in such a configuration is calculated and compared with that arising under the same conditions of loading when the fibers are infinite in length.

In Section 1 of the present paper we formulate the two problems with which we are concerned using the procedure of Sternberg and Muki. The principal result in Section 1 is an integro-differential equation governing the distribution of axial force in the filaments. This integro-differential equation is reduced to a Fredholm integral equation in Section 2. In Section 3 we utilize this integral equation to determine the asymptotic distribution of axial filament force far from the ends of the filaments in the twin-filament problem (Problem 1). We also determine in Section 3 the singular asymptotic behavior of the filament-matrix bond force near the ends of the filaments for Problem 1. Section 4 is devoted to the numerical technique and results for the twin-filament problem, while the overlapping-filament problem is analyzed asymptotically and numerically in Section 5.

1. Formulation of the problem.

In this section we shall formulate both problems and derive the basic equations which govern the distribution of load in each filament. With this objective in mind we introduce the following notation (see Figures 1 and 2). In terms of rectangular Cartesian coordinates x_1, x_2, x_3, the three-dimensional region occupied by filament 1 is the semi-infinite right circular cylinder of radius a, described by $0 \le x_1^2 + x_2^2 \le a^2$, $x_3 \ge 0$. In Problem 1 (the twin problem) filament 2 occupies the semi-infinite cylinder $0 \le x_1^2 + (x_2 - \ell)^2 \le a^2$, $x_3 \ge 0$, while in Problem 2 (the overlap problem), filament 2 lies in the region $0 \le x_1^2 + (x_2 - \ell)^2 \le a^2$, $-\infty < x_3 \le h$. Thus in both problems, the filament axes are separated by a distance ℓ; it is assumed throughout that $\ell \ge 2a$. In Problem 2, h stands for the overlap; $-\infty < h < \infty$. In both problems we denote by R the open region occupied by the two filaments; thus R is the union of two parallel semi-infinite cylinders. We note that the origin of coordinates is at the center of the end of filament 1.

In order that we may treat the two problems simultaneously, we find it convenient to introduce the following additional notation. Let $\underset{\sim}{s}$ be the vector from the origin to the center of the end section of filament 2; thus $\underset{\sim}{s} = (0, \ell, d)$, where $d = 0$ in Problem 1, but $d = h$ in Problem 2. Moreover, let $\underset{\sim}{y}$ be a unit vector in the direction of the axis of filament 2, so that $\underset{\sim}{y} = (0, 0, j)$, where in Problem 1, $j = 1$, while in Problem 2, $j = -1$. Finally denote by Π_z^1 the closed circular disc $x_1^2 + x_2^2 \le a^2$, $x_3 = z$, $-\infty < z < \infty$. Similarly let Π_z^2 stand for the disc

$x_1^2 + (x_2 - \ell)^2 \leq a^2$, $x_3 = d + jz$, $-\infty < z < \infty$. It is important to note that if $z \geq 0$, Π_z^1, Π_z^2 are the cross-sections at a distance z from the ends of filament 1 and filament 2, respectively.

It is assumed that the materials comprising both matrix and filaments are homogeneous, isotropic and elastic. For the matrix material, E_1 and ν stand for Young's modulus and Poisson's ratio, respectively. For the filament material, Young's modulus is denoted by E_2. In the approximate treatment to be employed here, Poisson's ratio for the filament material does not enter the analysis. We restrict our attention to pairs of materials for which $E_2 > E_1 > 0$ and $-1 < \nu < 1/2$. This is the case for all composite materials of practical interest.

We are now in a position to introduce the approximation scheme used by Muki and Sternberg [3], [4] in their analysis of single-filament problems. According to this scheme, the actual filaments are replaced by fictitious ones of Young's modulus $E_2 - E_1$, and the extended matrix (modulus E_1) is then assumed to occupy all space. Thus the region R is simultaneously occupied by two elastic materials, one with modulus E_1 (the matrix) and one with modulus $E_2 - E_1$ (the filaments). In the subsequent analysis the three-dimensional linear theory of elasticity is assumed to apply everywhere in the extended matrix, but the fictitious filaments are treated as one-dimensional.

Suppose α is either 1 or 2 and consider a cross-section Π_z^α in filament α. We assume that an axial force $p_*^\alpha(z)$ is transmitted by fictitious filament α across Π_z^α; $p_*^\alpha(z)$ is positive if it is tensile. In

addition, it is assumed that each fictitious filament is acted upon by a "bond force" per unit length $q_*^\alpha(z)$ arising from the presence of the extended matrix. This bond force is positive if it points in the direction of increasing z. In order to maintain equilibrium in each fictitious filament we require that p_*^α, q_*^α satisfy

$$\frac{d}{dz} p_*^\alpha(z) + q_*^\alpha(z) = 0 \quad , \quad 0 < z < \infty \; ; \tag{1.1}$$

The stress-strain relations for the fictitious filaments are taken in the form

$$\frac{1}{\pi a^2} p_*^\alpha(z) = (E_2 - E_1) e_*^\alpha(z) \quad , \quad 0 \le z < \infty \; , \tag{1.2}$$

where $e_*^\alpha(z)$ is the extensional strain in fictitious filament α, and a is the cross-section radius.

Let $\underset{\sim}{e}_i$ stand for the unit normal vectors associated with the Cartesian frame. Then in the extended matrix we suppose that the stress and strain tensor fields — denoted respectively by $\underset{\sim}{\sigma}(\underset{\sim}{x})$, $\underset{\sim}{\varepsilon}(\underset{\sim}{x})$ — arise according to the equations of the linear theory of elasticity* from the following sources: (1) the stress $\overset{\infty}{\underset{\sim}{\sigma}}$ prescribed at infinity, (2) body forces distributed uniformly over Π_z^α whose resultants over Π_z^1 and Π_z^2 are respectively $q_*^1(z)\underset{\sim}{e}_3$ and $q_*^2(z)\underset{\sim}{y}$, (3) terminal bond forces distributed uniformly over Π_o^α whose resultants over Π_z^1 and Π_z^2 are respectively $p_*^1(0)\underset{\sim}{e}_3$ and $p_*^2(0)\underset{\sim}{y}$.

Throughout the present work the prescribed stress at infinity is taken to be uniaxial tension in the x_3-direction.

---

*We omit the explicit statement of these equations.

The final ingredient required for the determination of the fields of interest in the fictitious filament – extended matrix mixture is the bond condition. It is required that the axial strain $e_*^\alpha(z)$ in the fictitious filament coincide with the average over Π_z^α of the component ϵ_{33} of the strain tensor $\underset{\sim}{\epsilon}$ in the extended matrix. Thus

$$e_*^\alpha(z) = \frac{1}{\pi a^2} \int_{\Pi_z^\alpha} \epsilon_{33}\, dA \quad , \quad 0 \le z < \infty \, . \tag{1.3}$$

Once the field quantities $p_*^\alpha, q_*^\alpha, e_*^\alpha, \underset{\sim}{\sigma}, \underset{\sim}{\epsilon}$ have been determined, the axial force distribution in an actual filament can be calculated from p_*^α and σ_{33}. In view of the superposition of fictitious filaments and extended matrix which forms the basis of the present model, the axial force $p^\alpha(z)$ exerted across Π_z^α in actual filament α is taken to be

$$p^\alpha(z) = p_*^\alpha(z) + \int_{\Pi_z^\alpha} \sigma_{33}\, dA \quad , \quad 0 \le z < \infty \, . \tag{1.4}$$

This completes the description of the model to be used in the present analysis.

The solution of the field equations described above is substantially simplified by the symmetry present in both Problems 1 and 2. Since in both cases the load at infinity is uniaxial tension, symmetry immediately yields

$$\left.\begin{aligned} & p_*^1(z) = p_*^2(z) \equiv p_*(z) \\ \text{and} \qquad & \\ & p^1(z) = p^2(z) \equiv p(z) \quad , \quad 0 \le z < \infty \end{aligned}\right\} \tag{1.5}$$

in both problems.

Following Muki and Sternberg [3, 4], the first step in the reduction of the problem as formulated above is based on Kelvin's solution to the concentrated force problem in linear elastostatics [7] and leads to an integro-differential equation for the fictitious filament load $p_*(z)$. For all $\underset{\sim}{x} \neq \underset{\sim}{0}$, let $\overset{\circ}{\underset{\sim}{\sigma}}(\underset{\sim}{x}; \underset{\sim}{m})$, $\overset{\circ}{\underset{\sim}{\varepsilon}}(\underset{\sim}{x}; \underset{\sim}{m})$ be the stress and strain tensor fields, respectively, arising from a concentrated force of unit magnitude acting at $\underset{\sim}{x} = \underset{\sim}{0}$ in the direction $-\underset{\sim}{m}$, where $\underset{\sim}{m}$ is a unit vector*. By superposition,

$$\left.\begin{aligned} \hat{\underset{\sim}{\sigma}}(\underset{\sim}{x}; \underset{\sim}{m}) &= \frac{1}{\pi a^2} \int_{\Pi_o^1} \overset{\circ}{\underset{\sim}{\sigma}}(\underset{\sim}{x}-\underset{\sim}{y}; \underset{\sim}{m})\, dA_y \\ \hat{\underset{\sim}{\varepsilon}}(\underset{\sim}{x}; \underset{\sim}{m}) &= \frac{1}{\pi a^2} \int_{\Pi_o^1} \overset{\circ}{\underset{\sim}{\varepsilon}}(\underset{\sim}{x}-\underset{\sim}{y}; \underset{\sim}{m})\, dA_y \end{aligned}\right\} \underset{\sim}{x} \notin \Pi_o^1 . \tag{1.6}$$

represent stress and strain tensor fields satisfying the equations of linear elastostatics for all $\underset{\sim}{x}$ not in Π_o^1 and correspond to a body force uniformly distributed over the disc Π_o^1 whose resultant has unit magnitude. The functions $\hat{\underset{\sim}{\sigma}}$ and $\hat{\underset{\sim}{\varepsilon}}$ have jump discontinuities across Π_o^1.

By a further superposition it follows that the stress tensor $\underset{\sim}{\sigma}(\underset{\sim}{x})$ and the strain tensor $\underset{\sim}{\varepsilon}(\underset{\sim}{x})$ arising in the extended matrix from the load at infinity $\overset{\infty}{\underset{\sim}{\sigma}}$, the bond forces $-q_*^\alpha$ and the terminal bond forces $p_*^\alpha(0)$ are given by

$$\underset{\sim}{\sigma}(\underset{\sim}{x}) = \overset{\infty}{\underset{\sim}{\sigma}} - p_*^1(0)\hat{\underset{\sim}{\sigma}}(\underset{\sim}{x}; \underset{\sim}{e}_3) - p_*^2(0)\hat{\underset{\sim}{\sigma}}(\underset{\sim}{x}-\underset{\sim}{s}; \underset{\sim}{v}) + \int_0^\infty q_*^1(z)\hat{\underset{\sim}{\sigma}}(\underset{\sim}{x}-z\underset{\sim}{e}_3; \underset{\sim}{e}_3)\, dz$$

$$+ \int_0^\infty q_*^2(z)\hat{\underset{\sim}{\sigma}}(\underset{\sim}{x}-\underset{\sim}{s}-z\underset{\sim}{v}; \underset{\sim}{v})\, dz , \qquad \underset{\sim}{x} \notin \Pi_o^1 + \Pi_o^2 , \tag{1.7}$$

---

*The direction $-\underset{\sim}{m}$, rather than $\underset{\sim}{m}$, is chosen so that our notation and and sign conventions will conform to those in [3].

$$\underset{\sim}{\varepsilon}(\underset{\sim}{x}) = \overset{\infty}{\underset{\sim}{\varepsilon}} - p_*^1(0)\hat{\underset{\sim}{\varepsilon}}(\underset{\sim}{x}; \underset{\sim}{e}_3) - p_*^2(0)\hat{\underset{\sim}{\varepsilon}}(\underset{\sim}{x}-\underset{\sim}{s}; \underset{\sim}{v}) + \int_0^\infty q_*^1(z)\hat{\underset{\sim}{\varepsilon}}(\underset{\sim}{x}-z\underset{\sim}{e}_3; \underset{\sim}{e}_3)\,dz$$

$$+ \int_0^\infty q_*^2(z)\hat{\underset{\sim}{\varepsilon}}(\underset{\sim}{x}-\underset{\sim}{s}-z\underset{\sim}{v}; \underset{\sim}{v})\,dz, \quad x \notin \Pi_o^1 + \Pi_o^2 . \qquad (1.8)$$

For reference purposes we give here the formulas for $\overset{\infty}{\underset{\sim}{\sigma}}, \overset{\infty}{\underset{\sim}{\varepsilon}}$, which are merely the stress and strain fields corresponding to a state of uniaxial tension of magnitude σ_o in an isotropic, homogeneous medium according to linear elastostatics:

$$\overset{\infty}{\sigma}_{ij} = \delta_{i3}\delta_{j3}\sigma_o \quad , \quad \overset{\infty}{\varepsilon}_{ij} = \frac{\sigma_o}{E_1}\left[(1+\nu)\delta_{3i}\delta_{3j} - \nu\delta_{ij}\right]; \qquad (1.9)$$

δ_{ij} is the Kronecker delta.

To obtain the integro-differential equation for p_*, we first express q_*^1, q_*^2 in (1.7), (1.8) in terms of p_* by means of the filament equilibrium equations (1.1) and the symmetry relation (1.5). The component ε_{33} of the strain tensor provided by (1.8) is then substituted into the bond condition (1.3) to obtain the filament strain $e_*(z) \equiv e_*^1(z) = e_*^2(z)$ in terms of $\overset{\infty}{\varepsilon}$, $p_*(0)$, and $(d/dz)p_*(z)$. This in turn is substituted into the filament stress-strain relation (1.2) to obtain the integro-differential equation. The result of these steps can be written in the form

$$p_*(z) = \pi a^2(E_2 - E_1)\left\{\frac{\sigma_o}{E_1} - p_*(0)\,\varepsilon(z, 0) - jp_*(0)\,\varepsilon(z-d, \ell)\right.$$

$$\left. - \int_0^\infty \varepsilon(z-t, 0)\frac{d}{dt}[p_*(t)]dt - j\int_0^\infty \varepsilon(z-d-jt, \ell)\frac{d}{dt}[p_*(t)]dt\right\}, \quad 0 < z < \infty .$$

(1.10)

Here

$$j = 1\ ,\ d = 0 \text{ in Problem 1}\ ; \qquad j = -1\ ,\ d = h \text{ in Problem 2} \tag{1.11}$$

and the kernel function $\epsilon(z, L)$ is defined as follows:

$$\epsilon(z, L) = \frac{1}{\pi a^2} \int_{\Pi_z^1} \hat{\epsilon}_{33}(\underset{\sim}{x} - L\underset{\sim}{e}_2\ ;\ \underset{\sim}{e}_3)\, dA_{\underset{\approx}{x}}\ , \quad z \neq 0\ ,\ L \geq 0\ . \tag{1.12}$$

In (1.12), $\hat{\epsilon}_{33}$ is given in terms of Kelvin's strain field by the second of (1.6).

Once $p_*(z)$ is determined from (1.10), the <u>actual</u> filament load $p(z)$ is found from (1.4), (1.7), (1.1) as follows:

$$\begin{aligned} p(z) = p_*(z) + \pi a^2 \Big\{ & \sigma_o - p_*(0)\sigma(z, 0) - j p_*(0)\sigma(z-d, \ell) \\ & - \int_0^\infty \sigma(z-t, 0) \frac{d}{dt}[p_*(t)]\, dt \\ & - j \int_0^\infty \sigma(z-d-jt, \ell) \frac{d}{dt}[p_*(t)]\, dt \Big\}, \quad 0 < z < \infty\ , \end{aligned} \tag{1.13}$$

where

$$\sigma(z, L) = \frac{1}{\pi a^2} \int_{\Pi_z^1} \hat{\sigma}_{33}(\underset{\sim}{x} - L\underset{\sim}{e}_2\ ,\ \underset{\sim}{e}_3)\, dA_{\underset{\approx}{x}}\ , \quad z \neq 0\ ,\ L \geq 0. \tag{1.14}$$

Although strictly speaking the case $E_2 = E_1$ has been excluded, it may be noted that (1.10), (1.13) <u>formally</u> yield

$$p_*(z) = 0\ , \quad p(z) = \pi a^2 \sigma_o\ , \quad 0 < z < \infty\ , \tag{1.15}$$

if we set $E_2 = E_1$.

As a final remark concerning the formulation of our problems we note that the fictitious filament load at $z = \infty$ is not prescribed in

advance, but rather is determined from (1.2), (1.3) and (1.9) to be

$$p_*(\infty) = \pi a^2 \sigma_o \frac{E_2 - E_1}{E_1} . \tag{1.16}$$

The actual filament load at $z = \infty$ is then found from (1.16), (1.4) and (1.9) to be

$$p(\infty) = \pi a^2 \sigma_o \frac{E_2}{E_1} . \tag{1.17}$$

We turn next to the analysis of the integro-differential equation (1.10).

2. Reduction to a Fredholm integral equation.

In this section we will transform the integro-differential equation (1.10) and the formula (1.13) for the filament load into more convenient forms for further analysis*. We begin by obtaining explicit representations for the kernels ϵ and σ defined in (1.12) and (1.14).

The axial strain and stress components associated with the classical solution due to Kelvin [7] for the problem of a concentrated force of unit magnitude in the $-x_3$ direction acting at the origin are

$$\left.\begin{aligned} \mathring{\epsilon}_{33}(\underset{\sim}{x};\underset{\sim}{e}_3) &= -\frac{1+\nu}{8\pi(1-\nu)E_1}\left[2(1-2\nu)\frac{\partial}{\partial x_3}\left(\frac{1}{|\underset{\sim}{x}|}\right) - x_3\frac{\partial^2}{\partial x_3^2}\left(\frac{1}{|\underset{\sim}{x}|}\right)\right], \\ \mathring{\sigma}_{33}(\underset{\sim}{x};\underset{\sim}{e}_3) &= -\frac{1}{8\pi(1-\nu)}\left[2(1-\nu)\frac{\partial}{\partial x_3}\left(\frac{1}{|\underset{\sim}{x}|}\right) - x_3\frac{\partial^2}{\partial x_3^2}\left(\frac{1}{|\underset{\sim}{x}|}\right)\right], \end{aligned}\right\} \quad (2.1)$$

$$\underset{\sim}{x} \neq 0.$$

In order to obtain ϵ and σ from (1.12), (1.14), we must first substitute (2.1) into (1.6) to obtain the auxiliary functions $\hat{\sigma}$ and $\hat{\epsilon}$. After a suitable interchange of integration and differentiation, this furnishes

$$\left.\begin{aligned} \hat{\epsilon}_{33}(\underset{\sim}{x};\underset{\sim}{e}_3) &= \frac{1+\nu}{8\pi(1-\nu)E_1}\left[2(1-2\nu)\frac{\partial}{\partial x_3}U(\underset{\sim}{x}) - x_3\frac{\partial^2}{\partial x_3^2}U(\underset{\sim}{x})\right], \\ \hat{\sigma}_{33}(\underset{\sim}{x};\underset{\sim}{e}_3) &= \frac{1}{8\pi(1-\nu)}\left[2(1-\nu)\frac{\partial}{\partial x_3}U(\underset{\sim}{x}) - x_3\frac{\partial^2}{\partial x_3^2}U(\underset{\sim}{x})\right], \end{aligned}\right\} \quad x_3 \neq 0. \quad (2.2)$$

where for all $\underset{\sim}{x}$,

*Much of the analysis in the present section is an extension of that contained in [8].

$$U(\underset{\sim}{x}) = -\frac{1}{\pi a^2}\int_{\Pi_o^1}\frac{dA_{\underset{\sim}{y}}}{|\underset{\sim}{x}-\underset{\sim}{y}|} = -\frac{1}{\pi a^2}\int_{\Pi_o^1}\frac{dA_{\underset{\sim}{y}}}{\left[(x_1-y_1)^2+(x_2-y_2)^2+x_3^2\right]^{1/2}}\,. \quad (2.3)^*$$

Let

$$W(z,L) = \frac{1}{\pi a^2}\int_{\Pi_z^1} U(\underset{\sim}{x}-L\underset{\sim}{e}_2)\,dA_{\underset{\sim}{x}}\,, \quad L\geq 0\,, \text{ all } z. \quad (2.4)$$

Then (1.12), (1.14), (2.2) and (2.4) yield

$$\left.\begin{aligned}\epsilon(z,L) &= \frac{1+\nu}{8\pi(1-\nu)E_1}\left[2(1-2\nu)\frac{\partial}{\partial z}W(z,L) - z\frac{\partial^2}{\partial z^2}W(z,L)\right],\\ \sigma(z,L) &= \frac{1}{8\pi(1-\nu)}\left[2(1-\nu)\frac{\partial}{\partial z}W(z,L) - z\frac{\partial^2}{\partial z^2}W(z,L)\right],\end{aligned}\right\} z\neq 0\,,\ L\geq 0. \quad (2.5)$$

In order to obtain a more explicit representation for U, and hence for W, we employ the formula**

$$\int_0^\infty e^{-|x_3|s} J_o\left\{s\left[r^2+\rho^2-2r\rho\cos(\theta-\varphi)\right]^{1/2}\right\}ds = \left[(x_1-y_1)^2+(x_2-y_2)^2+x_3^2\right]^{-1/2}, \quad x_3\neq 0\,, \quad (2.6)$$

where J_o is the Bessel function of the first kind of order zero, and

$$x_1 = r\cos\theta\,,\quad x_2 = r\sin\theta\,,\quad y_1 = \rho\cos\varphi\,,\quad y_2 = \rho\sin\varphi\,. \quad (2.7)$$

Thus from (2.3), (2.6)

$$U(\underset{\sim}{x}) = -\frac{1}{\pi a^2}\int_0^a\int_0^{2\pi}\int_0^\infty e^{-|x_3|s} J_o\left\{s\left[r^2+\rho^2-2r\rho\cos(\theta-\varphi)\right]^{1/2}\right\}\rho\,ds\,d\varphi\,d\rho\,, \quad x_3\neq 0\,. \quad (2.8)$$

*Although (2.3) is an improper integral for $x_3=0$, it can be shown that $U(\underset{\sim}{x})$ is continuous at $x_3=0$.

**See Watson [9], p. 384.

We now employ the identity*

$$J_o\left\{s\left[r^2+\rho^2-2r\rho\cos(\theta-\varphi)\right]^{1/2}\right\} = J_o(sr)J_o(s\rho) + 2\sum_{k=1}^{\infty} J_k(sr)J_k(s\rho)\cos k(\theta-\varphi) \quad (2.9)$$

in (2.8), interchange the φ- and s- integrations, and integrate the series termwise with respect to φ. A final interchange or r- and s- integrations gives

$$U(\underset{\sim}{x}) = -\frac{2}{a^2}\int_0^{\infty}\int_0^{a} e^{-|x_3|s} J_o(sr)J_o(s\rho)\rho\, d\rho\, ds, \quad x_3 \neq 0,$$

or

$$U(\underset{\sim}{x}) = -\frac{2}{a}\int_0^{\infty} e^{-|x_3|s} J_o(sr)\frac{J_1(as)}{s}\, ds, \quad x_3 \neq 0, \quad r=\sqrt{x_1^2+x_2^2}. \quad (2.10)^{**}$$

Using (2.10) in (2.4) yields, upon interchange of integration,

$$W(z,L) = -\frac{2}{\pi a^2}\int_0^{\infty} e^{-|z|s}\frac{J_1(as)}{as}\int_{\Pi_z^1} J_o\left(s\sqrt{x_1^2+(x_2-L)^2}\right) dA_{\underset{\sim}{x}}\, ds,$$

$$z \neq 0, \quad L \geq 0. \quad (2.11)$$

The integral over Π_z^1 in (2.11) can again be evaluated with the aid of (2.9). It is found that

$$\int_{\Pi_z^1} J_o\left(s\sqrt{x_1^2+(x_2-L)^2}\right) dA_{\underset{\sim}{x}} = 2\pi\frac{a}{s}J_1(as)J_o(sL), \quad (2.12)$$

---

*See Watson [9], p. 358.

**This representation for the Newtonian potential of a disc carrying a uniformly distributed mass is due to Weber [10].

so that

$$W(z,L) = -4\int_0^\infty \frac{1}{(as)^2} e^{-|z|s} J_1^2(as)J_o(Ls)\,ds\,, \quad -\infty<z<\infty\,, \quad L\geq 0\,. \quad (2.13)^*$$

Prior to substituting (2.13) into (2.5), we introduce some convenient auxiliary functions as follows. Define

$$\Lambda_n(\zeta,\mu) = \int_0^\infty t^{n-2} e^{-\zeta t} J_1^2(t)J_o(\mu t)\,dt\,,$$
$$\zeta>0\,, \quad \mu\geq 0\,, \quad n=0,1,2,3\,. \quad (2.14)$$

It is easily observed that

$$\dot{\Lambda}_n(\zeta,\mu)\equiv \frac{\partial \Lambda_n}{\partial \zeta}(\zeta,\mu) = -\Lambda_{n+1}(\zeta,\mu)\,. \quad (2.15)$$

From (2.13), (2.14)

$$W(z,L) = -4\Lambda_o\left(\frac{|z|}{a}, \frac{L}{a}\right), \quad -\infty<z<\infty\,, \quad L\geq 0\,. \quad (2.16)$$

Combining (2.16), (2.15) and (2.5) yields the representations

$$\left.\begin{aligned}\epsilon(z,L) &= \frac{1+\nu}{2(1-\nu)E_1\pi a^2}\left[2(1-2\nu)(\operatorname{sgn} z)\Lambda_1\left(\frac{|z|}{a}, \frac{L}{a}\right) + \frac{z}{a}\Lambda_2\left(\frac{|z|}{a}, \frac{L}{a}\right)\right],\\ \sigma(z,L) &= \frac{1}{2(1-\nu)\pi a^2}\left[2(1-\nu)(\operatorname{sgn} z)\Lambda_1\left(\frac{|z|}{a}, \frac{L}{a}\right) + \frac{z}{a}\Lambda_2\left(\frac{|z|}{a}, \frac{L}{a}\right)\right],\end{aligned}\right\}$$
$$z\neq 0\,, \quad L\geq 0\,. \quad (2.17)$$

In the sequel we shall need the values of $\epsilon(0+, L)$, $\sigma(0+, L)$ for $L=0$ and for $L\geq 2a$. Suppose first $L\geq 2a$. From (2.14) it then follows that

$$\Lambda_1\left(0+, \frac{L}{a}\right) = \int_0^\infty \frac{J_1^2(t)}{t} J_o\left(\frac{L}{a}t\right)dt\,, \quad L\geq 2a\,. \quad (2.18)$$

---

*Although $z=0$ was excluded in deriving (2.13), the extension of this result for W at $z=0$ is easily carried out by continuity.

$$\Lambda_2\left(0+, \frac{L}{a}\right) = \int_0^\infty J_1^2(t)\, J_o\left(\frac{L}{a}\, t\right) dt\,, \quad L \geq 2a\,. \tag{2.19}$$

We thus have

$$\frac{\partial \Lambda_1}{\partial L}\left(0+, \frac{L}{a}\right) = -\frac{1}{a}\int_0^\infty J_1^2(t)\, J_1\left(\frac{L}{a}t\right) dt\,, \quad L \geq 2a\,. \tag{2.20}$$

The integral on the right can be evaluated with the aid of a special case of a formula due to Sonine (see Eq. (3), p. 411 of [9]):

$$\int_0^\infty J_1^2(t)\, J_1(ct)\, dt = 0 \quad \text{if} \quad c \geq 2\,. \tag{2.21}$$

It then follows from (2.20), (2.21) that $\Lambda_1\left(0+, \frac{L}{a}\right)$ is constant for $L \geq 2a$. But by the analog of the Riemann-Lebesgue lemma for Fourier-Bessel integrals (see [9], p. 457), $\Lambda_1\left(0+, \frac{L}{a}\right) \to 0$ as $L \to \infty$. We conclude that

$$\Lambda_1\left(0+, \frac{L}{a}\right) = 0 \text{ for } L \geq 2a\,. \tag{2.22}$$

Since $\Lambda_2\left(0+, \frac{L}{a}\right)$ is finite by (2.19), we conclude from an inspection of (2.17), (2.22) that

$$\varepsilon(0+, L) = \sigma(0+, L) = 0 \quad \text{for} \quad L \geq 2a\,. \tag{2.23}$$

Now consider the case $L = 0$. From (2.14) we have

$$\Lambda_n(\zeta, 0) = \int_0^\infty t^{n-2}\, e^{-\zeta t}\, J_1^2(t)\, dt\,, \quad \zeta > 0\,. \tag{2.24}$$

These integrals were expressed in terms of complete elliptic integrals in [3] using results obtained in [11]. If $K(k)$, $E(k)$ are the complete elliptic integrals of the first and second kinds, respectively, the formulas in [3] furnish, for $0 < \zeta < \infty$,

$$\left.\begin{aligned}
\Lambda_0(\zeta,0) &= -\frac{\zeta}{2} + \frac{4}{3\pi k}E(k) + \frac{\zeta^2}{3\pi k}[K(k)-E(k)]\,,\\
\Lambda_1(\zeta,0) &= \frac{1}{2} - \frac{\zeta}{\pi k}[K(k)-E(k)]\,,\\
\Lambda_2(\zeta,0) &= -\frac{k}{\pi}K(k) + \frac{2}{\pi k}[K(k)-E(k)]\,,\\
\Lambda_3(\zeta,0) &= \frac{k}{\pi\zeta}E(k) - \frac{k\zeta}{2\pi}[K(k)-E(k)]\,,
\end{aligned}\right\} \tag{2.25}$$

where

$$k \equiv k(\zeta) = \frac{2}{\sqrt{4+\zeta^2}}\,, \quad 0<\zeta<\infty\,. \tag{2.26}$$

From these formulas and the properties

$$E(1) = 1\,, \quad \lim_{k\to 1}\left[K(k) - \frac{1}{2}\log\frac{16}{1-k^2}\right] = 0\,, \tag{2.27}$$

there follows

$$\left.\begin{aligned}
\Lambda_o(\zeta,0) &= \frac{4}{3\pi} + o(1)\,,\\
\Lambda_1(\zeta,0) &= \frac{1}{2} + o(1)\,,\\
\Lambda_2(\zeta,0) &= -\frac{1}{\pi}\left[\log\frac{\zeta}{8}+2\right] + o(1)\,,\\
\Lambda_3(\zeta,0) &= \frac{1}{\pi\zeta} + o(1)\,,
\end{aligned}\right\} \text{ as } \zeta\to 0+\,. \tag{2.28}$$

From (2.28), (2.17) we obtain in particular

$$\lim_{z\to 0+}\epsilon(z,0) = \frac{(1-2\nu)(1+\nu)}{2(1-\nu)\pi a^2 E_1}\,, \quad \lim_{z\to 0+}\sigma(z,0) = \frac{1}{2\pi a^2}\,. \tag{2.29}$$

It may be remarked that $\epsilon(z,L)$, $\sigma(z,L)$ are odd functions of z which are continuously differentiable for all z if $L \geq 2a$; $\epsilon(z,0)$ and $\sigma(z,0)$ are continuously differentiable for $z \neq 0$ but have jump

discontinuities at z=0. This is to be expected in view of the physical meaning of $\epsilon(z,0)$, $\sigma(z,0)$.

We now turn to the derivation of the Fredholm integral equation to which (1.10) is equivalent. Let

$$\zeta = \frac{z}{a}$$

be a dimensionless filament coordinate and define a dimensionless filament separation distance λ by

$$\lambda = \frac{\ell}{a} . \tag{2.30}$$

Further, set

$$\left.\begin{aligned} \Delta_*(\zeta, \lambda) &= 1 - \frac{p_*(z)}{p_*(\infty)} , \\ \Delta(\zeta, \lambda) &= 1 - \frac{p(z)}{p(\infty)} , \end{aligned}\right\} \quad z \geq 0 , \ \zeta \geq 0 , \ \lambda \geq 2 \tag{2.31}$$

in which $p_*(\infty)$, $p(\infty)$ are given by (1.16), (1.17), respectively. In (2.31) we have indicated explicitly the dependence of Δ_* and Δ on the (dimensionless) separation constant λ. Note that Δ_* and Δ are expected to be small for large ζ. If the first of (2.31) is used to express $p_*(z)$ in (1.10) in terms of Δ_*, the integral in (1.10) may be integrated by parts to remove the derivative of Δ_*. (The discontinuity in $\epsilon(z,0)$ at $z = 0$ must be borne in mind during this process.) The result is

$$\left[\frac{1}{\pi a^2 (E_2 - E_1)} + 2\epsilon(0,0)\right] \Delta_*(\zeta, \lambda) = \epsilon(a\zeta, 0) + j\epsilon(a\zeta - d, a\lambda)$$

$$- a\int_0^\infty \Delta_*(\tau, \lambda)\left[\dot{\epsilon}(a\zeta - a\tau, 0) + \dot{\epsilon}(a\zeta - d - ja\tau, a\lambda)\right] d\tau, \quad 0 \leq \zeta \leq \infty. \tag{2.32}$$

where, according to (1.11),

$$j=1,\ d=0 \text{ in Problem 1}\ ,\quad j=-1,\ d=h \text{ in Problem 2}\ . \tag{2.33}$$

The kernel $\dot{\epsilon}$ is given by the first of (2.17), and

$$\dot{\epsilon}(z,L) \equiv \frac{\partial \epsilon}{\partial z}(z,L)\ . \tag{2.34}$$

If we set

$$\eta = \frac{d}{a}\ ,\quad \gamma = \frac{E_2}{E_1}\ ,\quad \omega = \frac{(1+\nu)(1-2\nu)}{1-\nu} \tag{2.35}$$

and introduce the functions

$$\left.\begin{aligned} K(\zeta,\mu) &= -\pi a^3 E_1 \dot{\epsilon}(a\zeta,a\mu)\ , \qquad \zeta \neq 0\ ,\ \mu \geq 0 \\ f(\zeta,\mu) &= \pi a^2 E_1 \epsilon(a\zeta,a\mu)\ , \qquad -\infty<\zeta<\infty\ ,\ \mu \geq 0 \end{aligned}\right\} \tag{2.36}$$

the integral equation (2.32) can be written in the form

$$\left(\omega+\frac{1}{\gamma-1}\right)\Delta_*(\zeta,\lambda) = f(\zeta,0)+jf(\zeta-\eta,\lambda)$$

$$+\int_0^\infty \Delta_*(\tau,\lambda)[K(\zeta-\tau,0)+K(\zeta-\eta-j\tau,\lambda)]\,d\tau\ ,\quad 0\leq\zeta<\infty\ ,\ 2\leq\lambda<\infty\ . \tag{2.37}$$

This is the integral equation to be solved for $\Delta_*(\zeta,\lambda)$.

Once $\Delta_*(\zeta,\lambda)$ is determined, $\Delta(\zeta,\lambda)$ is found from an integral formula derived from (1.13) by an argument analogous to that used above to obtain (2.37) from (1.10). The result is

$$\frac{\gamma}{\gamma-1}\Delta(\zeta,\lambda) = g(\zeta,0)+jg(\zeta-\eta,\lambda)$$

$$+\int_0^\infty \Delta_*(\tau,\lambda)[\mathcal{K}(\zeta-\tau,0)+\mathcal{K}(\zeta-\eta-j\tau,\lambda)]\,d\tau\ ,\quad 0\leq\zeta<\infty\ ,\ 2\leq\lambda<\infty\ , \tag{2.38}$$

where

$$\left.\begin{aligned} \mathcal{K}(\zeta,\mu) &= -\pi a^3 \dot{\sigma}(a\zeta, a\mu)\,, \quad \zeta \neq 0\,,\ \mu \geq 0\,, \\ g(\zeta,\mu) &= \pi a^2 \sigma(a\zeta, a\mu)\,, \quad -\infty < \zeta < \infty\,,\ \mu \geq 0\,, \end{aligned}\right\} \tag{2.39}$$

and

$$\dot{\sigma}(z,L) = \frac{\partial \sigma}{\partial z}(z,L)\,. \tag{2.40}$$

The functions K, L, f and g can be expressed in terms of the functions Λ_n by means of (2.17), (2.15). Thus it follows

$$\left.\begin{aligned} K(\zeta,\mu) &= \frac{1+\nu}{2(1-\nu)}\left[(1-4\nu)\Lambda_2(|\zeta|,\mu) + |\zeta|\Lambda_3(|\zeta|,\mu)\right], \\ \mathcal{K}(\zeta,\mu) &= \frac{1}{2(1-\nu)}\left[(1-2\nu)\Lambda_2(|\zeta|,\mu) + |\zeta|\Lambda_3(|\zeta|,\mu)\right], \end{aligned}\right\} \quad \zeta \neq 0\,,\ \mu \geq 0\,, \tag{2.41}$$

$$\left.\begin{aligned} f(\zeta,\mu) &= \frac{1+\nu}{2(1-\nu)}\left[2(1-2\nu)(\operatorname{sgn}\zeta)\Lambda_1(|\zeta|,\mu) + \zeta\Lambda_2(|\zeta|,\mu)\right], \\ g(\zeta,\mu) &= \frac{1}{2(1-\nu)}\left[2(1-\nu)(\operatorname{sgn}\zeta)\Lambda_1(|\zeta|,\mu) + \zeta\Lambda_2(|\zeta|,\mu)\right], \end{aligned}\right\} \quad -\infty < \zeta < \infty\,,\ \mu \geq 0\,. \tag{2.42}$$

3. Asymptotic analysis of the twin problem.

In this section the asymptotic behavior for large and small z of the filament force p(z) is determined for Problem 1 (the twin problem). We begin with an analysis appropriate to large z.

As a necessary preliminary step we first derive the asymptotic form of the relative load deviation Δ_* for the fictitious filament (see (2.31)). Since it is desirable that the asymptotic approximation for p be uniform in the dimensionless separation distance λ, we find it convenient to introduce the following notation. Let $\varphi(\zeta,\mu)$ be a function defined for $\zeta>0$ and $\mu\geq\mu_o$. For any real number n we shall write

$$\varphi(\zeta,\mu) = O_u(\zeta^n) \text{ as } \zeta\to\infty$$

if there exist constants M and ζ_o (both independent of μ) such that

$$|\varphi(\zeta,\mu)|\leq M\zeta^n \text{ for } \zeta\geq\zeta_o,\ \mu\geq\mu_o .$$

Similarly we write

$$\varphi(\zeta,\mu) = o_u(\zeta^n) \text{ as } \zeta\to\infty$$

if $\zeta^{-n}\varphi(\zeta,\mu)$ tends to zero as ζ tends to infinity, uniformly in μ for $\mu\geq\mu_o$. When the subscript u is omitted from the order symbols O, o, it is understood that the relevant asymptotic estimate holds merely for each fixed $\mu\geq\mu_o$.

In order to study the asymptotics of the integral equation (2.37) for Δ_* and the integral representation (2.38) for Δ, it is first necessary to find the behavior for large ζ of the kernels K, $\mathcal{K}$ and the functions f, g occurring in these equations. According to (2.41), (2.42) this can be done once the corresponding information concerning $\Lambda_n(\zeta,\mu)$ is obtained.

From (2.14)

$$\Lambda_n(\zeta,\mu) = \int_0^\infty t^{n-2} e^{-\zeta t} J_1^2(t) J_o(\mu t)\, dt\,, \quad \zeta>0\,,\ \mu\geq 0\,,\ n=0,1,2,3\,. \tag{3.1}$$

Since

$$J_1^2(t) = \frac{t^2}{4} + r(t)\,, \quad t\geq 0\,,$$

where, for some constant $k>0$ and for all $t\geq 0$,

$$|r(t)| \leq kt^4\,, \tag{3.2}$$

we may write (3.1) as

$$\Lambda_n(\zeta,\mu) = \frac{1}{4}\int_0^\infty t^n e^{-\zeta t} J_o(\mu t)dt + R_n(\zeta,\mu) \tag{3.3}$$

where

$$R_n(\zeta,\mu) = \int_0^\infty t^{n-2} e^{-\zeta t} r(t) J_o(\mu t)\, dt\,, \quad \zeta>0\,,\ \mu\geq 0\,. \tag{3.4}$$

Now (3.2), (3.4) and the fact that $|J_o(\mu t)|\leq 1$ for all $t\geq 0$, $\mu\geq 0$ furnish the estimate

$$|R_n(\zeta,\mu)| \leq k\int_0^\infty t^{n+2} e^{-\zeta t} dt = \frac{k(n+2)!}{\zeta^{n+3}}\,. \tag{3.5}$$

It follows that

$$\Lambda_n(\zeta,\mu) = \frac{1}{4}\int_0^\infty t^n e^{-\zeta t} J_o(\mu t)dt + O_u(\zeta^{-n-3}) \text{ as } \zeta\to\infty \text{ for } \mu\geq 0\,. \tag{3.6}$$

The integral in (3.6) can be evaluated* to give the following results.

---

*See [12], p. 182.

$$\left.\begin{aligned}
\Lambda_1(\zeta,\mu) &= \frac{1}{4\zeta^2}\left(1+\frac{\mu^2}{\zeta^2}\right)^{-3/2} + O_u(\zeta^{-4}) , \\
\Lambda_2(\zeta,\mu) &= \frac{1}{2\zeta^3}\left(1-\frac{1}{2}\frac{\mu^2}{\zeta^2}\right)\left(1+\frac{\mu^2}{\zeta^2}\right)^{-5/2} + O_u(\zeta^{-5}) , \\
\Lambda_3(\zeta,\mu) &= \frac{3}{2\zeta^4}\left(1-\frac{3}{2}\frac{\mu^2}{\zeta^2}\right)\left(1+\frac{\mu^2}{\zeta^2}\right)^{-7/2} + O_u(\zeta^{-6}) ,
\end{aligned}\right\} \text{ as } \zeta\to\infty . \qquad (3.7)$$

Thus the estimates (3.7) are uniform in μ for $\mu \geq 0$.

From (3.7), (2.41), (2.42) we next find

$$\left.\begin{aligned}
f(\zeta,\mu) &= \frac{1+\nu}{2\zeta^2}\left[1+\frac{1-4\nu}{4(1-\nu)}\frac{\mu^2}{\zeta^2}\right]\left(1+\frac{\mu^2}{\zeta^2}\right)^{-5/2} + O_u(\zeta^{-4}) , \\
g(\zeta,\mu) &= \frac{2-\nu}{4(1-\nu)\zeta^2}\left[1+\frac{1-2\nu}{2(2-\nu)}\frac{\mu^2}{\zeta^2}\right]\left(1+\frac{\mu^2}{\zeta^2}\right)^{-5/2} + O_u(\zeta^{-4}) , \\
K(\zeta,\mu) &= O_u(\zeta^{-3}) , \\
\mathcal{K}(\zeta,\lambda) &= O_u(\zeta^{-3}) ,
\end{aligned}\right\} \qquad (3.8)$$

as $\zeta\to\infty$, $\mu \geq 0$.

We now turn to an asymptotic analysis of the integral equation (2.37). Our procedure makes use of an approach which was developed by Muki and Sternberg [13] for the asymptotic analysis of a class of integral equations. For Problem 1, reference to (2.33), (2.35) shows that the integral equation (2.37) reduces to

$$\left(\omega+\frac{1}{\gamma-1}\right)\Delta_*(\zeta,\lambda) = f(\zeta,0)+f(\zeta,\lambda)+\int_0^\infty \Delta_*(\tau,\lambda)[K(\zeta-\tau,0)+K(\zeta-\tau,\lambda)]\,d\tau\,,$$

$$0\le\zeta<\infty\,,\ \lambda\ge 2\,. \qquad (3.9)$$

We assume the existence of a solution Δ_* of (3.9) with the following properties.

(i) For each $\lambda\ge 2$, $\Delta_*(\zeta,\lambda)$ is continuously differentiable in ζ for $\zeta>0$; $\lim_{\zeta\to 0+}\Delta_*(\zeta,\lambda)$ exists.

(ii) There is a constant M, independent of λ, such that

$$|\Delta_*(\zeta,\lambda)|\le M\,,\quad \zeta\ge 0\,,\ \lambda\ge 2\,. \qquad (3.10)$$

(iii) There exist a $\varkappa>0$ and a function $\delta(\zeta,\lambda)$ such that

$$\left.\begin{aligned}\Delta_*(\zeta,\lambda) &= \zeta^{-\varkappa}\delta(\zeta,\lambda)+o_u(\zeta^{-\varkappa})\,,\\ \frac{\partial\Delta_*}{\partial\zeta}(\zeta,\lambda) &= O_u(\zeta^{-\varkappa-1})\,,\end{aligned}\right\}\ \text{as } \zeta\to\infty \qquad (3.11)$$

where $\delta(\zeta,\lambda)$ is uniformly bounded for sufficiently large ζ and $\lambda\ge 2$, and the $\lim_{\zeta\to\infty}\delta(\zeta,\lambda)\ne 0$ for $\lambda\ge 2$.

Now consider the integral

$$I(\zeta,\lambda) = \int_0^\infty \Delta_*(\tau,\lambda)K(\zeta-\tau,\lambda)\,d\tau\,,\qquad \zeta\ge 0\,,\ \lambda\ge 2\,, \qquad (3.12)$$

and, for $\zeta>4$, decompose I as follows.

$$I = I_1+I_2+I_3+I_4\,, \qquad (3.13)$$

where

$$\left.I_1(\zeta,\lambda) = \int_0^{\sqrt{\zeta}} K(\zeta-\tau,\lambda)\Delta_*(\tau,\lambda)\,d\tau\,,\right\} \qquad (3.14)$$

$$\left.\begin{aligned} I_2(\zeta,\lambda) &= \int_{\sqrt{\zeta}}^{\zeta-\sqrt{\zeta}} K(\zeta-\tau,\lambda)\Delta_*(\tau,\lambda)\,d\tau\,, \\ I_3(\zeta,\lambda) &= \int_{\zeta-\sqrt{\zeta}}^{\zeta} K(\zeta-\tau,\lambda)\Delta_*(\tau,\lambda)\,d\tau\,, \\ I_4(\zeta,\lambda) &= \int_{\zeta}^{\infty} K(\zeta-\tau,\lambda)\Delta_*(\tau,\lambda)\,d\tau\,, \end{aligned}\right\} \quad \zeta \geq 4\,,\ \lambda \geq 2\,. \qquad (3.14)\ \text{cont.}$$

We shall show that, as $\zeta \to \infty$, I_3 and I_4 predominate in the asymptotic behavior of I. First consider I_1. From (3.10),

$$\begin{aligned} |I_1(\zeta,\lambda)| &\leq M \int_0^{\sqrt{\zeta}} |K(\zeta-\tau,\lambda)|\,d\tau \\ &\leq \sqrt{\zeta}\, M \max_{0\leq\tau\leq\sqrt{\zeta}} |K(\zeta-\tau,\lambda)| \\ &= \sqrt{\zeta}\, M \max_{\zeta-\sqrt{\zeta}\,\leq\tau\leq\zeta} |K(\tau,\lambda)|\,, \end{aligned}$$

so that, by the third of (3.8)

$$I_1(\zeta,\lambda) = O_u(\zeta^{-5/2}) \text{ as } \zeta\to\infty\,. \qquad (3.15)$$

In the second integral in (3.14) we make use of the first of (3.11) and the uniform boundedness of δ to write, for sufficiently large ζ,

$$|I_2(\zeta,\lambda)| \leq A_o \int_{\sqrt{\zeta}}^{\zeta-\sqrt{\zeta}} |K(\zeta-\tau,\lambda)|\,\tau^{-\varkappa}\,d\tau$$

for some constant A_o, independent of λ. From the third of (3.8) it follows that, for sufficiently large ζ,

$$|I_2(\zeta,\lambda)| \le A_1 \int_{\sqrt{\zeta}}^{\zeta-\sqrt{\zeta}} (\zeta-\tau)^{-3}\,\tau^{-\varkappa}\,d\tau\,, \tag{3.16}$$

where the constant A_1 is independent of λ. Estimation of the explicit integral in (3.16) then shows that

$$\left.\begin{aligned} &I_2(\zeta,\lambda) = o_u(\zeta^{-\varkappa}) \text{ if } 0<\varkappa\le 3\,,\\ &I_2(\zeta,\lambda) = o_u(\zeta^{-3}) \text{ if } \varkappa>3 \end{aligned}\right\} \quad \text{as } \zeta\to\infty\,. \tag{3.17}$$

For the integral I_3 in (3.14) a more detailed analysis is necessary. We set $\tau=\zeta-s$ and obtain

$$I_3(\zeta,\lambda) = \int_0^{\sqrt{\zeta}} K(s,\lambda)\Delta_*(\zeta-s,\lambda)\,ds$$

$$= \Delta_*(\zeta,\lambda)\int_0^{\sqrt{\zeta}} K(s,\lambda)ds + \int_0^{\sqrt{\zeta}} K(s,\lambda)[\Delta_*(\zeta-s,\lambda)-\Delta_*(\zeta,\lambda)]\,ds$$

or

$$I_3(\zeta,\lambda) = \Delta_*(\zeta,\lambda)\int_0^{\infty} K(s,\lambda)ds + J_3(\zeta,\lambda)\,, \tag{3.18}$$

where

$$J_3(\zeta,\lambda) = -\Delta_*(\zeta,\lambda)\int_{\sqrt{\zeta}}^{\infty} K(s,\lambda)ds + \int_0^{\sqrt{\zeta}} K(s,\lambda)[\Delta_*(\zeta-s,\lambda)-\Delta_*(\zeta,\lambda)]\,ds\,. \tag{3.19}$$

By virtue of the third of (3.8), the first of (3.11), and the uniform boundedness of δ, we conclude that the first term on the right in (3.19) is $o_u(\zeta^{-\varkappa})$ as $\zeta\to\infty$. Moreover,

$$\left|\int_0^{\sqrt{\zeta}} K(s,\lambda)[\Delta_*(\zeta-s,\lambda) - \Delta_*(\zeta,\lambda)]ds\right|$$

$$\leq \left\{\max_{0\leq s\leq\sqrt{\zeta}} |\Delta_*(\zeta-s,\lambda) - \Delta_*(\zeta,\lambda)|\right\}\int_0^{\infty} |K(s,\lambda)|ds$$

$$\leq \sqrt{\zeta}\max_{\zeta-\sqrt{\zeta}\leq s\leq\zeta} \left|\frac{\partial\Delta_*}{\partial\zeta}(s,\lambda)\right| \int_0^{\infty} |K(s,\lambda)|\,ds$$

$$\leq \left\{B_o\int_0^{\infty} |K(s,\lambda)|ds\right\} \zeta^{-\nu-\frac{1}{2}} ,$$

where the constant B_o is independent of λ, and use has been made of the mean value theorem of differential calculus and the second of (3.11). Further, $\int_0^{\infty} |K(s,\lambda)|ds$ can be shown to be uniformly bounded with the use of (2.41), (2.15), and (2.28) for $\lambda\geq 2$ and $-1<\nu<\frac{1}{2}$. It follows that

$$J_3(\zeta,\lambda) = o_u(\zeta^{-\nu}) \text{ as } \zeta\to\infty ,$$

and hence, from (3.18)

$$I_3(\zeta,\lambda) = \Delta_*(\zeta,\lambda)\int_0^{\infty} K(s,\lambda)ds + o_u(\zeta^{-\nu}) \text{ as } \zeta\to\infty . \tag{3.20}$$

An analysis similar to that applied to I_3 can be used to show that

$$I_4(\zeta,\lambda) = \Delta_*(\zeta,\lambda)\int_0^{\infty} K(s,\lambda)ds + o_u(\zeta^{-\nu}) \text{ as } \zeta\to\infty . \tag{3.21}$$

Combining (3.15), (3.17), (3.20), (3.21) in (3.13), (3.12) provides the useful formula

$$\int_0^{\infty} \Delta_*(\tau,\lambda)K(\zeta-\tau,\lambda)d\tau = 2\int_0^{\infty} K(\tau,\lambda)d\tau\,\Delta_*(\zeta,\lambda) + o_u(\zeta^{-\nu}) + o_u(\zeta^{-2})$$

$$\text{as } \zeta\to\infty,\ \lambda\geq 2 . \tag{3.21}$$

In an entirely similar way it may be shown that

$$\int_0^\infty \Delta_*(\tau,\lambda)K(\zeta-\tau,0)d\tau = 2\int_0^\infty K(\tau,0)d\tau\,\Delta_*(\zeta,\lambda) + o_u(\zeta^{-\varkappa}) + o_u(\zeta^{-2})$$

$$\text{as } \zeta\to\infty,\ \lambda\geq 2\,. \qquad (3.22)$$

The integrals of K appearing on the right in (3.21), (3.22) may be evaluated with the aid of the first of (2.36), (2.23), and the first of (2.29). Thus

$$\int_0^\infty K(\tau,0)\,d\tau = \omega/2\ , \quad \int_0^\infty K(\tau,\lambda)\,d\tau = 0\ , \quad \lambda\geq 2\,, \qquad (3.23)$$

where ω is given by (2.35). Using (3.23) in (3.21) and (3.22) we obtain

$$\int_0^\infty \Delta_*(\tau,\lambda)[K(\zeta-\tau,0)+K(\zeta-\tau,\lambda)]\,d\tau = \omega\Delta_*(\tau,\lambda) + o_u(\zeta^{-\varkappa}) + o_u(\zeta^{-2})$$

$$\text{as } \zeta\to\infty,\ \lambda\geq 2\,. \qquad (3.24)$$

We now return to the integral equation (3.9) and let $\zeta\to\infty$. It follows from (3.24) and (3.9) that $\Delta_*(\zeta,\lambda)$ satisfies

$$\left(\omega+\frac{1}{\gamma-1}\right)\Delta_*(\zeta,\lambda) = f(\zeta,0)+f(\zeta,\lambda)+\omega\Delta_*(\tau,\lambda)+o_u(\zeta^{-\varkappa})+o_u(\zeta^{-2})$$

$$\text{as } \zeta\to\infty,\ \lambda\geq 2\,. \qquad (3.25)$$

Substituting from the first of (3.11) into (3.25), we obtain

$$\delta(\zeta,\lambda) = (\gamma-1)\zeta^{\varkappa}[f(\zeta,0)+f(\zeta,\lambda)]+o_u(1)+o_u(\zeta^{\varkappa-2}) \text{ as } \zeta\to\infty,\ \lambda\geq 2\,. \qquad (3.26)$$

We now determine the value of $\varkappa$ as follows. Suppose first that $\varkappa>2$. Then (3.26) and the first of (3.8) show that $\delta(\zeta,\lambda)\to\infty$ as $\zeta\to\infty$, contradicting the boundedness of δ (Assumption (iii)). On the other hand, if $\varkappa<2$, (3.26) and the first of (3.8) can be seen to contradict the assumption $\lim_{\zeta\to\infty}\delta(\zeta,\lambda)\neq 0$. We conclude that

$$\varkappa = 2$$

and hence from (3.26), (3.11) that

$$\Delta_*(\zeta,\lambda) = (\gamma-1)[f(\zeta,0)+f(\zeta,\lambda)]+o_u(\zeta^{-2}) \text{ as } \zeta\to\infty,\ \lambda\geq 2\ . \tag{3.27}$$

It follows from (3.27) and (3.8) that

$$\Delta_*(\zeta,\lambda) = (\gamma-1)\frac{1+\nu}{2\zeta^2}\left\{1+\left[1+\frac{1-4\nu}{4(1-\nu)}\frac{\lambda^2}{\zeta^2}\right]\left(1+\frac{\lambda^2}{\zeta^2}\right)^{-5/2}\right\}+o_u(\zeta^{-2})$$

$$\text{as } \zeta\to\infty,\ \lambda\geq 2\ . \tag{3.28}$$

An argument analogous to that used above to derive the asymptotic representation (3.28) for Δ_* can be applied to (2.38) (specialized for Problem 1) to obtain the corresponding result for the relative load deviation Δ in the actual filament. The result of these computations is

$$\Delta(\zeta,\lambda) = (\gamma-1)\frac{1+\nu}{2\zeta^2}\left\{1-\frac{\nu(1-2\nu)}{2\gamma(1-\nu^2)}\right.$$

$$\left.+\left[1-\frac{\nu(1-2\nu)}{2\gamma(1-\nu^2)}+\frac{\lambda^2}{\zeta^2}\left\{\frac{1-4\nu}{4(1-\nu)}+\frac{\nu(1+4\nu)}{4\gamma(1-\nu^2)}\right\}\right]\left(1+\frac{\lambda^2}{\zeta^2}\right)^{-5/2}\right\}$$

$$+o_u(\zeta^{-2}) \text{ as } \zeta\to\infty,\ \lambda\geq 2\ . \tag{3.29}$$

The asymptotic formula (3.29), when combined with the definition (2.31) of $\Delta(\zeta,\lambda)$, furnishes the asymptotic behavior for large z of actual filament load p(z). In terms of the actual coordinate $z = a\zeta$ on the filaments, the actual separation distance ℓ, the filament radius a, and the two moduli E_1 and E_2, we have

$$\frac{p(z)}{p(\infty)} = 1 - \frac{E_2-E_1}{E_1}\,\frac{(1+\nu)}{2}\,\frac{a^2}{z^2}\left\{1 - \frac{E_1}{E_2}\,\frac{\nu(1-2\nu)}{2(1-\nu^2)}\right.$$

$$\left. + \left[1 - \frac{E_1}{E_2}\,\frac{\nu(1-2\nu)}{2(1-\nu^2)} + \frac{\ell^2}{z^2}\left\{\frac{1-4\nu}{4(1-\nu)} + \frac{E_1}{E_2}\,\frac{\nu(1+4\nu)}{4(1-\nu^2)}\right\}\right]\left(1+\frac{\ell^2}{z^2}\right)^{-5/2}\right\}$$

$$+ o_u(z^{-2}) \quad \text{as} \quad z\to\infty\,,\ \ell\geq 2a\,; \tag{3.30}$$

the uniformity in (3.30) refers to the parameter ℓ on the interval $\ell \geq 2a$. Recall from (1.17) that $p(\infty) = \pi a^2 \sigma_o E_2/E_1$. The asymptotic formula (3.30) for $p(z)$ is our principal result for large z in the twin filament problem.

If we set $\ell = \infty$ in the uniform estimate (3.30) we obtain

$$\frac{p(z)}{p(\infty)} = 1 - \frac{E_2-E_1}{E_1}\,\frac{1+\nu}{2}\left[1 - \frac{E_1}{E_2}\,\frac{\nu(1-2\nu)}{2(1-\nu^2)}\right]\frac{a^2}{z^2} + o_u(z^{-2}) \text{ as } z\to\infty. \tag{3.31}$$

Equation (3.31) is the result for a single filament obtained by Sternberg and Muki [3].

If ℓ is <u>fixed</u> in the interval $[2a, \infty)$, we obtain the <u>nonuniform</u> estimate

$$\frac{p(z)}{p(\infty)} = 1 - \frac{E_2-E_1}{E_1}(1+\nu)\left[1 - \frac{E_1}{E_2}\,\frac{\nu(1-2\nu)}{2(1-\nu^2)}\right]\frac{a^2}{z^2} + o(z^{-2})$$

$$\text{as } z\to\infty\ ,\ \ell \text{ fixed}\ ,\ 2a\leq\ell<\infty. \tag{3.32}$$

We note that the fixed-ℓ, two filament estimate (3.32) differs from the single filament result (3.31) only in that the coefficient $\frac{a^2}{z^2}$ in (3.32) is <u>twice</u> the corresponding coefficient in (3.31). It should also be observed that, according to (3.32), $p(z)/p(\infty)$ is independent of ℓ for

large z in the twin filament problem, up to and including terms of order z^{-2}.

In both the single and twin filament problems, $1 - p(z)/p(\infty)$ tends to zero like z^{-2}, and in both problems increases as the modulus ratio $\gamma = E_2/E_1$ increases for sufficiently large fixed z. Further comparisons between the single- and twin-filament problem will be deferred until the next section, which is devoted to a discussion of numerical results.

We turn briefly to the question of the behavior of p(z) for small z. While it does not seem possible to obtain p(0) directly from (2.38) and the second of (2.31), or (1.13), it is possible to determine the qualitative behavior of the derivative $\dot{p}(z)$ of p(z) as $z \to 0$. If to the Assumptions (i) - (iii), Page 27, concerning the solution $\Delta_*(z,\lambda)$ of the integral equation we add the additional assumption that, for some $k > 1$ and independent of λ, there exists a constant M, independent of λ, such that

$$\int_0^\infty \left| \frac{\partial \Delta_*}{\partial \zeta}(\zeta,\lambda) \right|^k d\zeta < M , \quad \lambda \geq 2 ,$$

it is possible to prove that $p(z,\ell)$ satisfies*

$$\frac{\partial p}{\partial z}(z,\ell) = \frac{1-2\nu}{2(1-\nu)\pi a} p_*(0,\ell) \log \frac{a}{z} + O(1) \text{ as } z \to 0+ , \qquad (3.33)$$

uniformly in ℓ, $\ell \geq 2a$. Apart from the potential dependence of $p_*(0,\ell)$ on ℓ, (3.33) is the same result obtained for the single filament

*In this section we have explicitly indicated the dependence of p and p_* on ℓ as well as z.

problem by Sternberg and Muki in [3]. The analysis required to establish (3.33) is similar in broad outline to that employed in [3] and will be omitted from the present work.

In view of the equilibrium equation (1.1) for the fictitious filaments, it is natural to regard

$$q(z,\ell) = -\frac{\partial p}{\partial z}(z,\ell)$$

as the bond force per unit length acting on an actual filament. The estimate (3.33) shows that this actual bond force becomes logarithmically infinite at the end of a filament unless $p_*(0,\ell) = 0$. Based on the numerical calculations to be described in the following section, $p_*(0,\ell)$ is not expected to vanish.

4. Numerical procedure for the calculation of the filament force. Discussion of results for Problem 1 (the twin problem).

A. Numerical procedure. To determine the distribution of the actual filament force for Problem 1, we must first solve the integral equation (3.9) for Δ_*. This solution is then utilized in the integral representation (2.38) for Δ, the relative filament force deviation (see (2.31)). A numerical procedure similar to that used by Sternberg and Muki [3] will be employed to calculate Δ_* and Δ. This procedure is described below.

As a preliminary step, it is necessary to establish an asymptotic estimate for the kernel K appearing in the integral equation (3.9). From (2.41) and (3.7) we find

$$K(\zeta,\mu) = \frac{1+\nu}{\zeta^3} + O(\zeta^{-5}) \quad \text{as} \quad \zeta\to\infty \quad , \quad \text{for each } \mu \geq 0 \quad . \tag{4.1}$$

We also recall the asymptotic behavior of the solution Δ_* of (3.9); according to (3.28),

$$\Delta_*(\zeta,\lambda) = \frac{\delta(\zeta,\lambda)}{\zeta^2} + o_u(\zeta^{-2}) \quad \text{as} \quad \zeta\to\infty \quad , \quad \lambda \geq 2 \, , \tag{4.2}$$

where

$$\delta(\zeta,\lambda) = (\gamma-1)\frac{1+\nu}{2}\left\{1+\left[1+\frac{1-4\nu}{4(1-\nu)}\frac{\lambda^2}{\zeta^2}\right]\left(1+\frac{\lambda^2}{\zeta^2}\right)^{-5/2}\right\} \quad . \tag{4.3}$$

Our analysis of the integral equation begins by writing (3.9), restricted to the interval $0 \leq \zeta \leq N$, in the form

$$\left(\omega+\frac{1}{\gamma-1}\right)\Delta_*(\zeta,\lambda) = f(\zeta,0)+f(\zeta,\lambda)$$
$$+\left\{\int_0^N+\int_N^{N+\zeta}+\int_{N+\zeta}^{\infty}\right\}\Delta_*(\tau,\lambda)[K(\zeta-\tau,0)+K(\zeta-\tau,\lambda)]\,d\tau\,,$$
$$0\le\zeta\le N\,. \qquad (4.4)$$

Here N is a positive number to be determined. For fixed large N the integral from $N+\zeta$ to ∞ in (4.4) is easily shown to be small by making use of (4.1), (4.2) and (4.3). This suggests truncating the integral equation (4.4) by dropping the term involving the integral from $N+\zeta$ to ∞. Moreover, in the integral from N to $N+\zeta$, we replace Δ_* by δ/ζ^2, making use of the fact that N is large. The integral equation which is to be solved numerically is thus

$$\left(\omega+\frac{1}{\gamma-1}\right)\hat{\Delta}_*(\zeta,\lambda) = f(\zeta,0)+f(\zeta,\lambda)+J(\zeta,\lambda)$$
$$+\int_0^N\hat{\Delta}_*(\tau,\lambda)[K(\zeta-\tau,0)+K(\zeta-\tau,\lambda)]\,d\tau\,,$$
$$0\le\zeta\le N\,, \qquad (4.5)$$

where f is given by the first of (2.42), and

$$J(\zeta,\lambda) = \int_N^{N+\zeta}\frac{\delta(\tau,\lambda)}{\tau^2}[K(\zeta-\tau,0)+K(\zeta-\tau,\lambda)]\,d\tau\,, \qquad (4.6)$$

in which δ is given in (4.3). In all calculations to be described below, it was found that $N=15\sqrt{\gamma-1}$ is suitable.

Let us now introduce a set of meshpoints $\{\zeta_i\}_{i=1}^{Q}$ which partition the interval $[0,N]$ where $0=\zeta_1<\zeta_2<\ldots<\zeta_Q=N$. Our objective is to approximate the integral equation in (4.5) by means of a set of linear algebraic equations for the values of $\hat{\Delta}_*(\zeta,\lambda)$ at the meshpoints. It will be necessary to evaluate the functions f and K that appear in (4.5) at

certain arguments associated with the meshpoints. Using (2.41) and (2.42), we can express $f(\zeta,\mu)$ and $K(\zeta,\mu)$ in terms of the functions $\Lambda_n(\zeta,\mu)(n=1,2,3)$ or, if $\mu=0$, in terms of the complete elliptic integrals using (2.25). Further, we can approximately evaluate $J(\zeta,\lambda)$ at every meshpoint $\zeta_i<N$ by applying the trapezoidal rule to (4.6). When $\zeta_i=N\,(i=\hat{Q})$, $K(\zeta-\tau,0)$ has a logarithmic singularity within the range of integration in (4.6) (see (2.41) and (2.28)). This singularity must first be extracted and integrated analytically before the trapezoidal rule is applied to the remainder of the integral.

The evaluation of the integral in (4.5) at a meshpoint ζ_i could be performed using the same technique as that described for the evaluation of J. However, it is possible to reduce the error in the numerical integration for a given set of meshpoints and eliminate the necessity of special treatment of the singularity in K by adopting a piecewise linear (or polygonal) approximation for $\hat{\Delta}_*$. The integration can then be performed analytically between each pair of meshpoints, making use of the identities,

$$\int_{\zeta_k}^{\zeta_i} K(s,\mu)\,ds = f(\zeta_k,\mu) - f(\zeta_i,\mu), \quad \mu \geq 0, \tag{4.7}$$

$$\int_{\zeta_k}^{\zeta_i} sK(s,\mu)\,ds = \beta(\zeta_k,\mu) - \beta(\zeta_i,\mu), \quad \mu \geq 0, \tag{4.8}$$

where f is known from (2.36) and

$$\beta(\zeta,\mu) = \frac{1+\nu}{2(1-\nu)}\left\{\zeta^2\Lambda_2(|\zeta|,\mu) + (3-4\nu)\left[\,|\zeta|\Lambda_1(|\zeta|,\mu) + \Lambda_o(|\zeta|,\mu)\right]\right\}. \tag{4.9}$$

Equation (4.9) follows from (2.41) and (2.15). This integration results

in a linear combination of the values $\hat{\Delta}_*(\zeta_i,\ell)$ so that (4.3) reduces to the following linear system of algebraic equations

$$\left[\frac{1}{\gamma-1}+\omega\right]\hat{\Delta}_*(\zeta_i,\lambda) = f(\zeta_i,0)+f(\zeta_i,\lambda)+J(\zeta_i,\lambda)$$

$$+\sum_{n=2}^{Q}\int_{\zeta_{n-1}}^{\zeta_n}(m_n\tau+b_n)\left[K(\zeta_i-\tau,0)+K(\zeta_i-\tau,\lambda)\right]d\tau\,, \quad \lambda\geq 2\,, \qquad (4.10)$$

where

$$m_n = \frac{\hat{\Delta}_*(\zeta_n,\lambda)-\hat{\Delta}_*(\zeta_{n-1},\lambda)}{\zeta_n-\zeta_{n-1}}\,, \quad b_n = \hat{\Delta}_*(\zeta_n,\lambda)-\zeta_n m_n\,. \qquad (4.11)$$

Once $\hat{\Delta}_*$ has been determined from (4.10) and (4.11), a similar numerical procedure can be applied to the integral representation (2.38) for Δ. Using the second of (2.31), we can finally compute the actual filament force p(z).

B. Results for the twin-filament problem. We now turn to a discussion of the numerical results for Problem 1 (the twin-filament problem). Figures 3 and 4 show the variation of the normalized filament force $p(z)/p(\infty)$ with distance along the filaments for separation distances $\ell = 2.2a$ and $\ell = 5a$, and for several different stiffness ratios γ. Poisson's ratio for the matrix has the value $\nu = 1/4$ throughout. Also plotted in these figures are the corresponding results for a single semi-infinite filament obtained by Muki and Sternberg [3] and reconfirmed by the present calculations. We note that the differences between the single-filament and the twin-filament cases are quite small even when the filaments are within one fifth of a radius of each

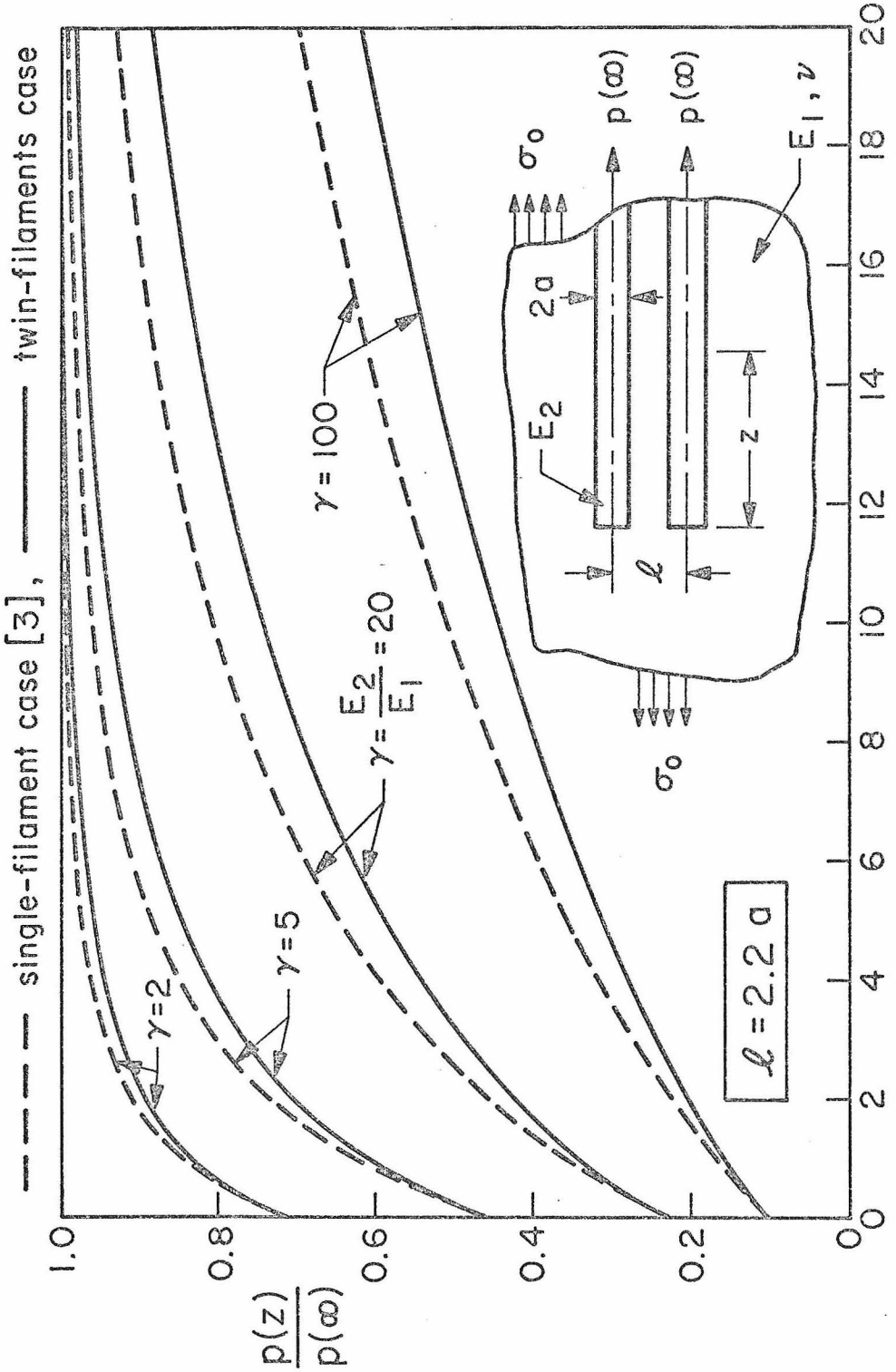

FIGURE 3. VARIATION OF FILAMENT-LOAD WITH DISTANCE ALONG FILAMENT, $\ell = 2.2\,a$.

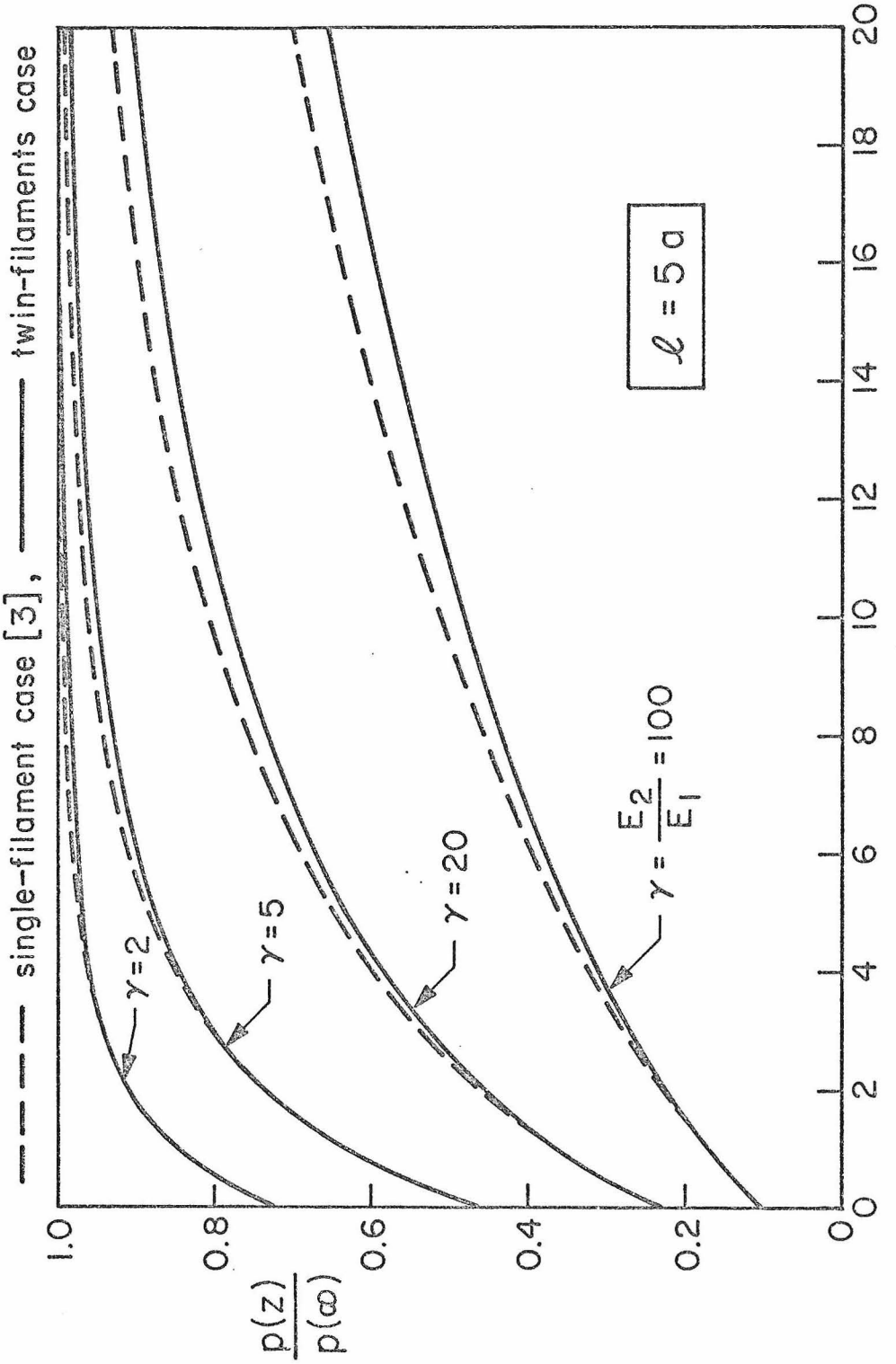

FIGURE 4. VARIATION OF FILAMENT-LOAD WITH DISTANCE ALONG FILAMENT, $\ell = 5a$.

other ($\ell = 2.2a$), Figure 3. The difference between the forces as compared to the forces themselves never exceeds 15% for the values of stiffness ratio considered here. These differences become smaller still as the separation distance ℓ increases. In fact, the single- and twin-filament cases are essentially indistinguishable for $\ell = 20a$ over the range of z/a and $\gamma = E_2/E_1$ covered in Figures 3 and 4.

We also observe from Figures 3 and 4 that $p(z)/p(\infty)$ does not vanish as z tends to zero. Thus a portion of the load absorbed by the filament is transmitted directly to its end. This portion of the absorbed load decreases with increasing stiffness ratio $\gamma = E_2/E_1$ as is clear from the figures under discussion.

Equation (3.33) predicts an infinite initial slope for all the curves in Figures 3 and 4, although the curves themselves do not clearly reveal this phenomenon with the existing scale. This infinite slope corresponds to infinite bond-force density at $z = 0$ and arises because of the assumptions of small elastic deformations and a perfect bond between filaments and matrix.

Varying Poisson's ratio for the matrix was found to produce an insignificant effect on the difference between the single- and twin-filament cases.

In Figure 5 the normalized filament force $p(z)/p(\infty)$ is again plotted as a function of position along the filament for $\ell = 2.2a$, but here we have included the uniform asymptotic results given in (3.30). For a given z the quality of the asymptotic approximation decrease as the stiffness ratio increases.

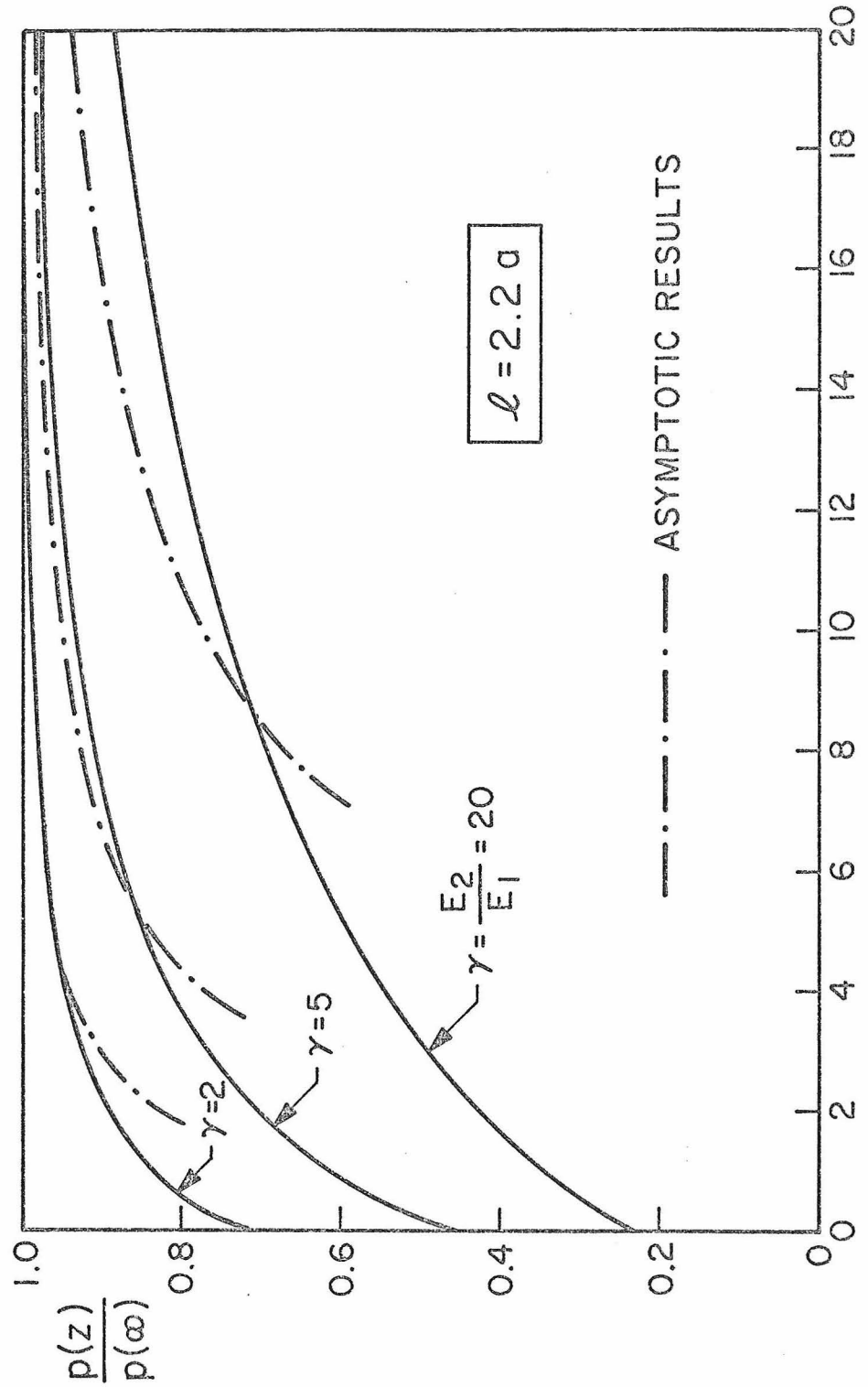

FIGURE 5. VARIATION OF FILAMENT-LOAD WITH DISTANCE ALONG FILAMENT, INCLUDING ASYMPTOTIC RESULTS.

Figure 6, which is based on a stiffness-dependent contracted length scale $z/a\sqrt{\gamma-1}$, reveals more explicitly how the stiffness ratio affects the rate at which $p(z)/p(\infty)$ approaches one.

In order to illustrate more clearly the previously noted small effect of varying ℓ, we have plotted the cases corresponding to $\ell = 2.2a$, 3a, 5a, 20a for $E_2/E_1 = 5$ and $E_2/E_1 = 100$ in Figures 7 and 8. The simple filament case also appears in these figures. In Figure 7 the curve for $\ell = 20a$ is omitted since it in fact coincides with the single-filament case. The value of $p(0)$ is apparently unaffected by the variation in ℓ, so that the force transmitted to the end of the filament would seem to be essentially the same in either the twin-filament or single-filament configuration for the ranges of the parameter appropriate to Figure 7.

The asymptotic force $p(\infty)$ which a filament carries is proportional to the filament stiffness. However, it is clear that the rate at which $p(z)/p(\infty)$ approaches one decreases as the stiffness ratio $\gamma = E_2/E_1$ increases. In order to quantify this more clearly and facilitate comparison corresponding results obtained in [3] for the single filament case, we introduce the characteristic length b through the requirement

$$p(b) = \frac{9}{10}\, p(\infty) .$$

In Figure 9 we have plotted b/a versus the stiffness ratio $\gamma = E_2/E_1$ for $\ell = 2.2a$, 3a, 5a, 20a and for the single filament case. It may be remarked that b is essentially linear in γ for $\gamma > 100$.

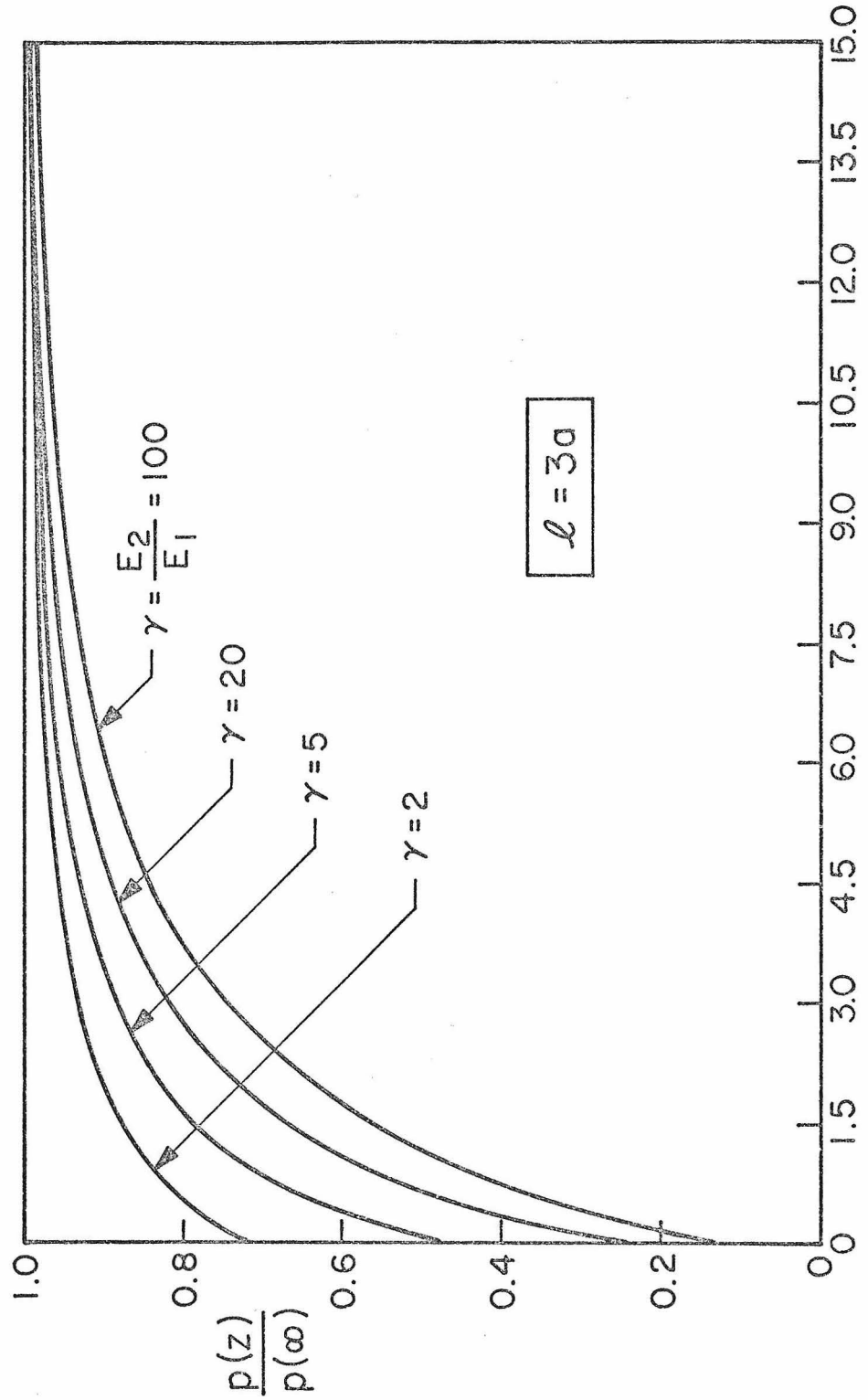

FIGURE 6. VARIATION OF FILAMENT-LOAD WITH CONTRACTED DISTANCE ALONG FILAMENT.

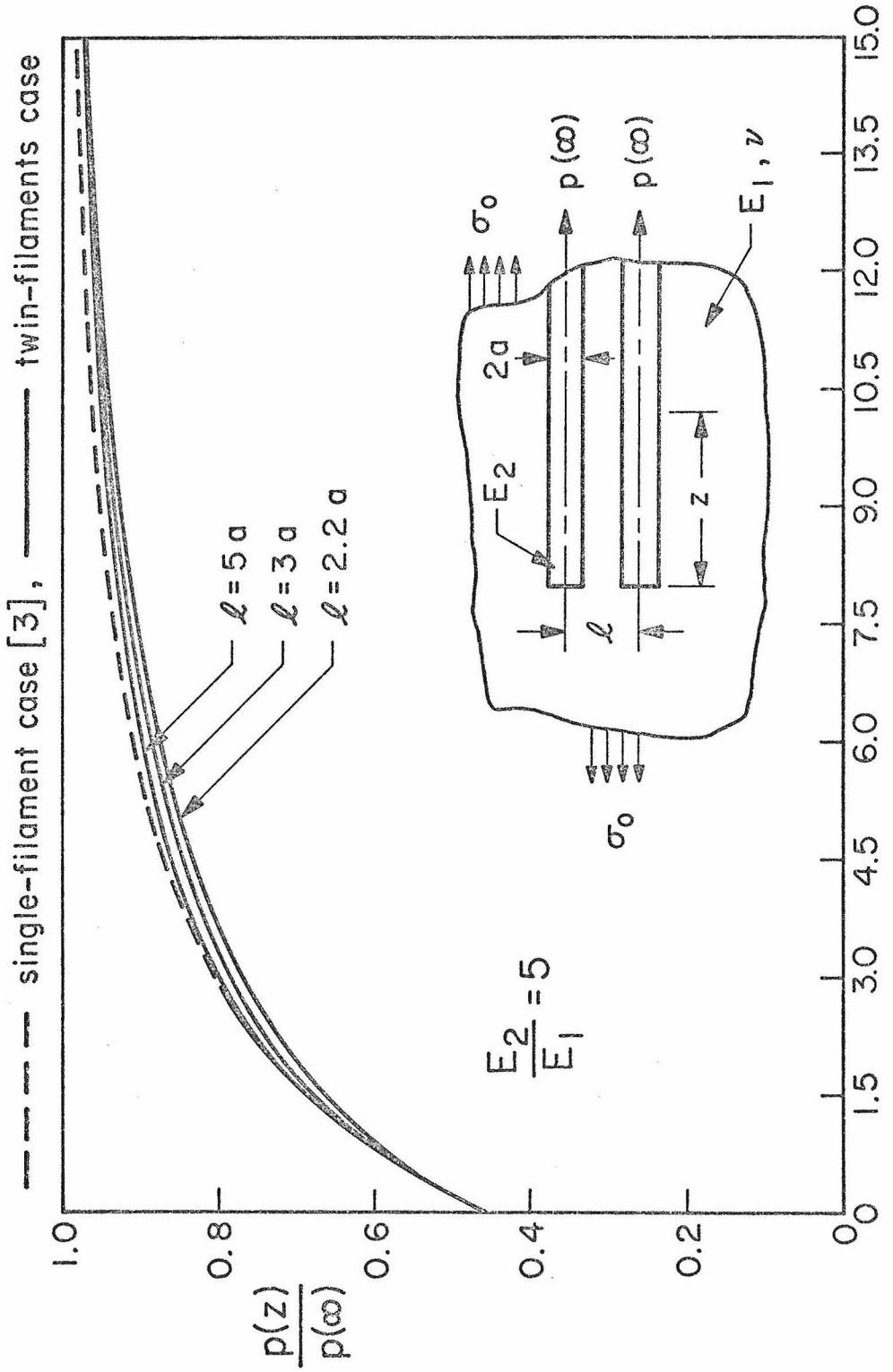

FIGURE 7. VARIATION OF FILAMENT-LOAD WITH DISTANCE ALONG FILAMENT, $E_2/E_1 = 5$.

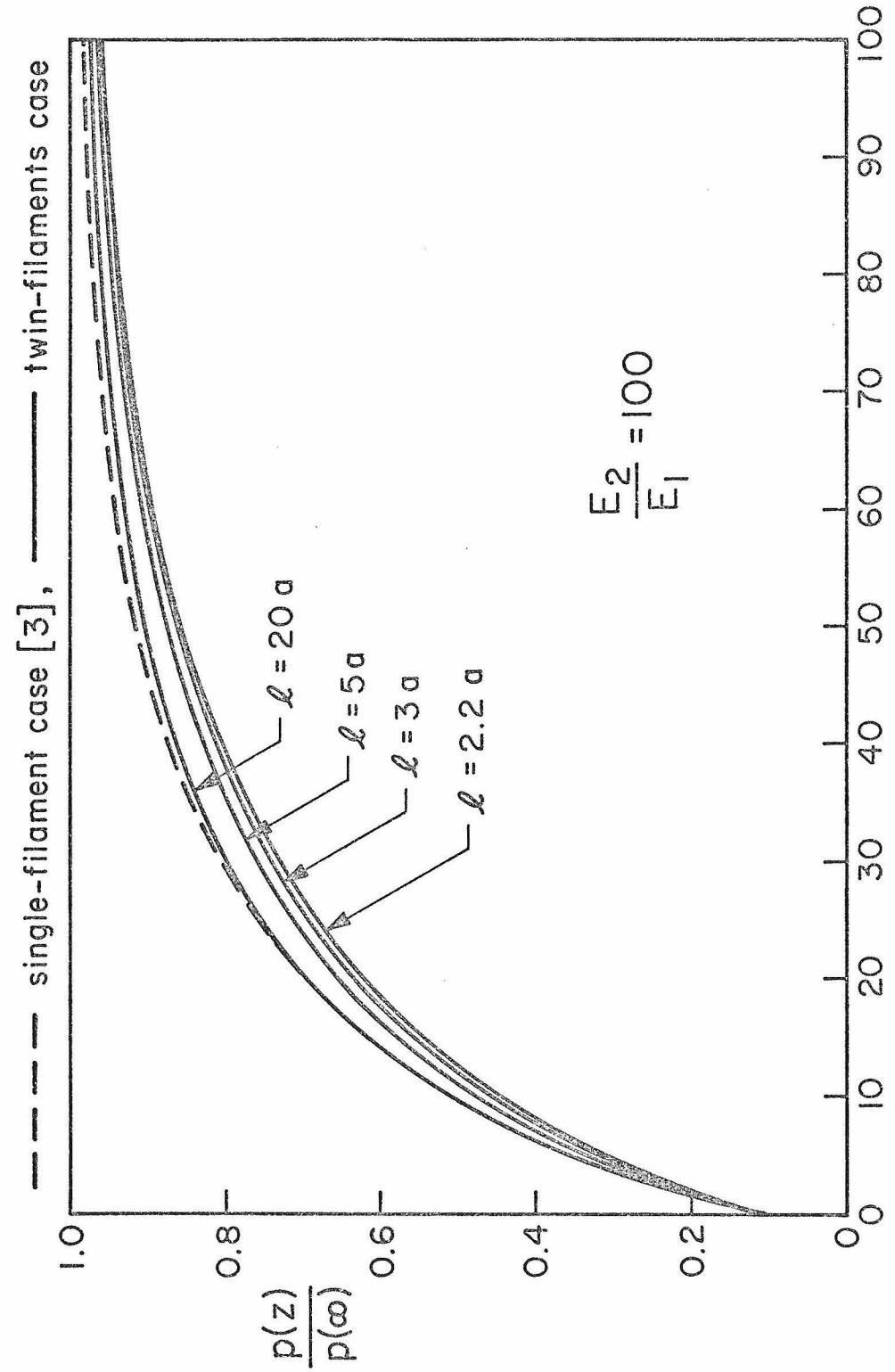

FIGURE 8. VARIATION OF FILAMENT-LOAD WITH DISTANCE ALONG FILAMENT, $E_2/E_1 = 100$.

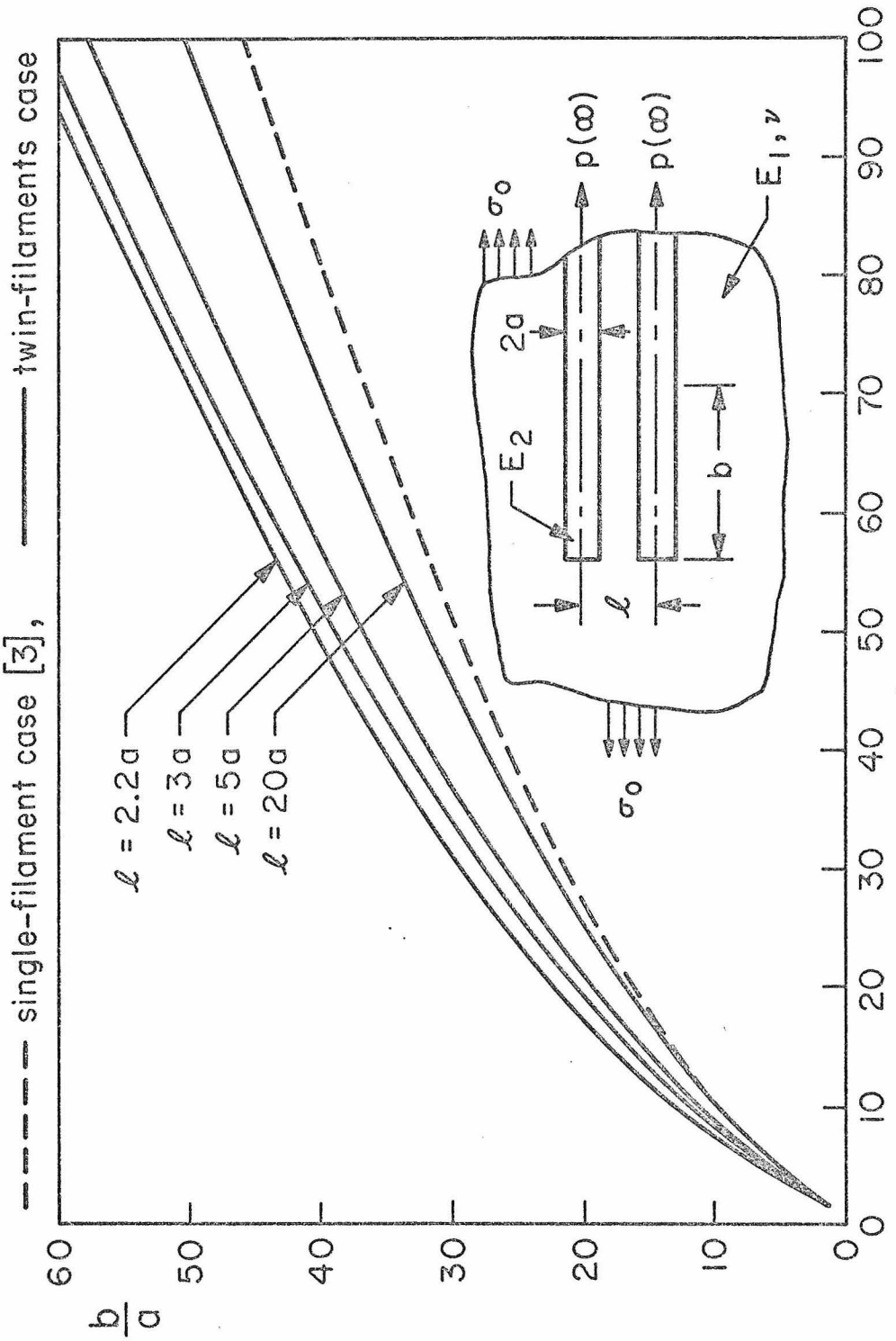

FIGURE 9. DEPENDENCE OF b/a ON STIFFNESS-RATIO, WHERE p(b)/p(∞) = 0.9.

5. Analysis and results for the overlap problem.

In this section the asymptotic character of the filament force p(z) for large and small z is determined for Problem 2 (the overlap problem). The numerical procedure employed in the overlap problem is briefly discussed, as are the associated numerical results.

A. Asymptotic analysis for large z. As in Section 3 our procedure makes use of an approach to the asymptotic analysis of a class of integral equations which was developed by Muki and Sternberg [13]. As a preliminary step to finding the asymptotic result for p(z), we first derive the asymptotic form of the relative load deviation Δ_* for the fictitious filament (see (2.31)). For Problem 2, reference to (2.33), (2.35) shows that the integral equation (2.37) reduces to

$$\left(\omega+\frac{1}{\gamma-1}\right)\Delta_*(\zeta) = f(\zeta,0) - f(\zeta-\eta,\lambda)+\int_0^\infty \Delta_*(\tau)[K(\zeta-\tau,0)+K(\zeta+\tau-\eta,\lambda)]\,d\tau$$

$$0\le\zeta<\infty\ ,\quad \lambda\ge 2\ ,\quad -\infty<\eta<\infty\ . \qquad (5.1)^*$$

While it does not seem possible to derive an asymptotic approximation for Δ_* which is uniform in λ and η, it is possible to deduce an asymptotic formula for fixed λ and η. We assume the existence of a solution Δ_* of (5.1) with the following properties for each λ and η:

(i) $\Delta_*(\zeta)$ is continuous for $\zeta\ge 0$.

(ii) There exists an $\alpha>0$ and a constant $c\neq 0$ such that

$$\Delta_*(\zeta) = \frac{c}{\zeta^\alpha}+o(\zeta^{-\alpha}) \quad \text{as} \quad \zeta\to\infty\ . \qquad (5.2)$$

---

*In the notation employed in this section, we have suppressed the dependence of Δ_* and Δ on the parameters λ and η, corresponding respectively to the dimensionless separation and overlap.

We shall proceed as in Section 3 by first determining the behavior for large ζ of the integral occurring in (5.1), and then deducing the asymptotic form of Δ_* by balance-of-terms in (5.1). Since parts of this asymptotic analysis are similar to that described in detail in Section 3, we shall only outline the corresponding steps.

Consider the integral

$$\mathcal{I}(\zeta) = \int_0^\infty \Delta_*(\tau)K(\zeta-\tau,0)\,d\tau \quad , \quad \zeta \geq 0 \, , \tag{5.3}$$

and for $\zeta > 4$, decompose $\mathcal{I}$ as follows.

$$\mathcal{I} = \mathcal{I}_1 + \mathcal{I}_2 + \mathcal{I}_3 + \mathcal{I}_4 \, , \tag{5.4}$$

where

$$\left.\begin{aligned} \mathcal{I}_1(\zeta) &= \int_0^{\sqrt{\zeta}} \Delta_*(\tau)K(\zeta-\tau,0)\,d\tau \, , \\ \mathcal{I}_2(\zeta) &= \int_{\sqrt{\zeta}}^{\zeta-\sqrt{\zeta}} \Delta_*(\tau)K(\zeta-\tau,0)\,d\tau \, , \\ \mathcal{I}_3(\zeta) &= \int_{\zeta-\sqrt{\zeta}}^{\zeta} \Delta_*(\tau)K(\zeta-\tau,0)\,d\tau \, , \\ \mathcal{I}_4(\zeta) &= \int_{\zeta}^{\infty} \Delta_*(\tau)K(\zeta-\tau,0)\,d\tau \, , \end{aligned}\right\} \quad \zeta > 4 \, . \tag{5.5}$$

The following estimates, valid for <u>fixed</u> λ and η, can be established by arguments similar to those presented in Section 3.

$$\mathcal{I}_1(\zeta) = o(\zeta^{-3}) \quad \text{as} \quad \zeta \to \infty \, . \tag{5.6}$$

$$\mathcal{J}_2(\zeta) = \begin{cases} K(\zeta,0)\int_0^\infty \Delta_*(\tau)\,d\tau + o(\zeta^{-3}) + o(\zeta^{-\alpha}) \text{ as } \zeta\to\infty \text{ , if } \alpha>1 \text{ ,} \\ o(\zeta^{-\alpha}) \text{ as } \zeta\to\infty \text{ , if } 0<\alpha\le 1 \text{ .} \end{cases} \tag{5.7}$$

$$\mathcal{J}_3(\zeta) = \Delta_*(\zeta)\int_0^\infty K(\tau,0)\,d\tau + o(\zeta^{-\alpha}) \text{ as } \zeta\to\infty . \tag{5.8}$$

$$\mathcal{J}_4(\zeta) = \Delta_*(\zeta)\int_0^\infty K(\tau,0)\,d\tau + o(\zeta^{-\alpha}) \text{ as } \zeta\to\infty . \tag{5.9}$$

Collecting (5.6), (5.7), (5.8), (5.9) in (5.4) provides the formulas

$$\left.\begin{aligned} \mathcal{J}(\zeta) &= 2\Delta_*(\zeta)\int_0^\infty K(\tau,0)\,d\tau + K(\zeta,0)\int_0^\infty \Delta_*(\tau)\,d\tau + o(\zeta^{-\alpha}) + o(\zeta^{-3}) \\ &\qquad \text{as } \zeta\to\infty \text{ , if } \alpha>1 , \\ \mathcal{J}(\zeta) &= 2\Delta_*(\zeta)\int_0^\infty K(\tau,0)\,d\tau + o(\zeta^{-3}) \quad \text{as } \zeta\to\infty \text{ , if } 0<\alpha\le 1 . \end{aligned}\right\} \tag{5.10}$$

The integrals of K appearing in (5.10) can be evaluated by using the first of (3.23),

$$\int_0^\infty K(\tau,0)\,d\tau = \frac{w}{2} . \tag{5.11}$$

The asymptotic behavior for large ζ of $\int_0^\infty \Delta_*(\tau)K(\zeta+\tau-\eta,\lambda)\,d\tau$ can be determined in a similar way, except that in this case we need only partition the range of integration into the two subintervals $[0,\sqrt{\zeta}]$ and $[\sqrt{\zeta},\infty)$. It may be shown that

$$\int_0^\infty \Delta_*(\tau)K(\zeta+\tau-\eta,\lambda)\,d\tau = \begin{cases} K(\zeta,0)\int_0^\infty \Delta_*(\tau)\,d\tau + o(\zeta^{-3}) + o(\zeta^{-\alpha}) & \text{if } \alpha>1\,, \\ o(\zeta^{-\alpha}) & \text{if } 0<\alpha\le 1\,, \end{cases}$$

$$\text{as } \zeta\to\infty\,. \qquad (5.12)$$

The first of (3.8) can be used to show that

$$f(\zeta,0) - f(\zeta-\eta,\lambda) = -\frac{1+\nu}{\zeta^3}\eta + O(\zeta^{-4}) \text{ as } \zeta\to\infty\,,$$

$$\text{for each fixed } \eta, \text{ fixed } \lambda\ge 2\,. \qquad (5.13)$$

We now return to the integral equation (5.1) and examine its behavior as $\zeta\to\infty$. Making use of (5.13), (5.12), (5.11), (5.10), (4.1) and (5.3), we find that (5.1) yields either

$$\left(\omega+\frac{1}{\gamma-1}\right)\Delta_*(\zeta) = -\frac{1+\nu}{\zeta^3}\eta + \omega\Delta_*(\zeta) + \frac{2(1+\nu)}{\zeta^3}\int_0^\infty \Delta_*(\tau)\,d\tau$$

$$+ o(\zeta^{-3}) + o(\zeta^{-\alpha}) \text{ as } \zeta\to\infty\,, \text{ if } \alpha>1\,, \qquad (5.13a)$$

or

$$\left(\omega+\frac{1}{\gamma-1}\right)\Delta_*(\zeta) = -\frac{1+\nu}{\zeta^3}\eta + \omega\Delta_*(\zeta) + o(\zeta^{-\alpha}) \text{ as } \zeta\to\infty\,,\ 0<\alpha\le 1\,. \qquad (5.13b)$$

Equations (5.13 a, b) now permit us to determine the exponent α in the asymptotic formula (5.2) for Δ_* provided Δ_* satisfies

$$2\int_0^\infty \Delta_*(\tau)\,d\tau - \eta \neq 0\,. \qquad (5.14)$$

If (5.14) holds, then (5.13 a, b) are easily shown to imply that

$$\alpha = 3\,, \quad c = (\gamma-1)(1+\nu)\left[2\int_0^\infty \Delta_*(\tau)\,d\tau - \eta\right]. \qquad (5.15)$$

If, on the other hand, (5. 14) is not satisfied, then (5. 13 a, b) only show that $\alpha > 3$.

It must be emphasized that the condition (5. 14) depends on a global property of the unknown solution $\Delta_*(\zeta)$ of (5. 1). Analytical efforts to determine whether (5. 14) holds have thus far been unsuccessful. At this stage we are therefore only able to make the following assertion about the asymptotic behavior of $\Delta_*(\zeta)$ for large ζ: For fixed η, $-\infty < \eta < \infty$, and fixed $\lambda \geq 2$,

$$\left.\begin{aligned} \Delta_*(\zeta) &= \frac{(\gamma-1)(1+\nu)}{\zeta^3}\left[2\int_0^\infty \Delta_*(\tau)\,d\tau - \eta\right] + o(\zeta^{-3}) \text{ as } \zeta\to\infty, \\ &\qquad \text{if } 2\int_0^\infty \Delta_*(\tau)\,d\tau - \eta \neq 0\,; \\ \Delta_*(\zeta) &= o(\zeta^{-3}) \text{ as } \zeta\to\infty \text{ if } 2\int_0^\infty \Delta_*(\tau)\,d\tau - \eta = 0\,. \end{aligned}\right\} \qquad (5.16)$$

There may be values of the various material and geometrical parameters which are such that (5. 14) fails. In such a case the second of (5. 16) shows that $\Delta_*(\zeta)$ tends to zero faster than ζ^{-3}; otherwise the first of (5. 16) holds. We have separated the two cases in (5. 16) only for emphasis; they can clearly be combined into the single statement

$$\Delta_*(\zeta) = (\gamma-1)\,\frac{(1+\nu)}{\zeta^3}\left[2\int_0^\infty \Delta_*(\tau)\,d\tau - \eta\right] + o(\zeta^{-3}) \text{ as } \zeta\to\infty, \qquad (5.17)$$

with no restriction like (5. 14).

An argument analogous to that used above to derive the asymptotic representation (5. 17) for Δ_* can be applied to (2. 38) (specialized for the overlap problem) to obtain the corresponding

result for the relative load deviation Δ in the actual filament. The result of this computation is

$$\Delta(\zeta) = \left(2\int_0^\infty \Delta_*(\tau)\,d\tau - \eta\right)\left[(\gamma-1)(1+\nu) + \frac{2-\nu}{2(1-\nu)}\right]\frac{\gamma-1}{\gamma}\,\frac{1}{\zeta^3} + o(\zeta^{-3}) \text{ as } \zeta\to\infty . \tag{5.18}$$

From this asymptotic result and the definition (2.31) of $\Delta(\zeta)$, the asymptotic character for large z of the actual filament force p(z) follows. Recalling that $z = a\zeta$, we have

$$\frac{p(z)}{p(\infty)} = 1 - \frac{\gamma-1}{\gamma}\left[(\gamma-1)(1+\nu) + \frac{2-\nu}{2(1-\nu)}\right]\frac{\gamma-1}{\gamma}\,\frac{a^3}{z^3}\left[2\int_0^\infty \Delta_*(\tau)\,d\tau - \eta\right]$$

$$+ o(z^{-3}) \text{ as } z\to\infty . \tag{5.19}$$

Once again the asymptotic formula (5.19) for $p(z)/p(\infty)$ involves the unknown integral of Δ_* over the interval $[0,\infty)$. While this diminishes the utility of the formula somewhat, it nevertheless remains useful in connection with the numerical procedure to be described in the sequel.

One important feature of the asymptotic representation (5.19) should be noted. The ratio $p(z)/p(\infty)$ may exceed unity for large z if $(2\int_0^\infty \Delta_*(\tau)\,d\tau - \eta)$ is negative. Thus (5.19) suggests the possibility that in the overlap problem the filament loads may exceed their values at infinity, in contrast to the situation in the twin-filament problem. This phenomenon is discussed further in connection with the numerical results.

B. Asymptotic analysis for small z. As in the twin-filament problem it does not appear to be possible to obtain p(0) analytically from (2.38) and the second of (2.31). On the other hand, an asymptotic estimate for small z of the derivative of p(z) — and hence of the bond force in the actual filament — can be obtained from (1.13) by an argument entirely analogous to that used in Section 3 to derive (3.33). If it is assumed that the solution Δ_* of the integral equation (5.1) has the property that

$$\int_0^\infty \left| \frac{d\Delta_*(\zeta)}{d\zeta} \right|^k d\zeta < \infty$$

for some constant $k > 1$, it is possible to prove that p(z) satisfies

$$\frac{dp(z)}{dz} = \frac{1-2\nu}{2(1-\nu)\pi a} p_*(0) \log \frac{a}{z} + O(1) \text{ as } z \to 0+ \quad , \quad h, \ell \text{ fixed}, \ell \geq 2a \, . \quad (5.20)$$

This is the same as the corresponding result (3.33) for Problem 1, except that $p_*(0)$ in (5.20) may depend on the overlap h as well as the separation ℓ. Moreover (5.20) may not hold uniformly with respect to h and ℓ.

C. Numerical procedure. The numerical scheme used to determine $\Delta_*(\zeta)$, $\Delta(\zeta)$ and p(z) in the present problem is essentially the same as that described in Part A of Section 4 for the twin filament problem. The integral appearing in (5.1) is again broken up into integrals over the subintervals $[0, N]$, $[N, N+\zeta]$ and $[N+\zeta, \infty)$, where N is large. The integral from $N+\zeta$ to ∞ is again discarded, and the integral from N to $N+\zeta$ is analyzed with the aid of the asymptotic estimate (5.17). The

integral from 0 to N is evaluated by means of a polygonal approximation procedure analogous to that used in connection with the approximate evaluation of the integral in (4.5).

The second step in this process — that of analyzing the integral from N to N+ζ — requires a more elaborate analysis than the corresponding step in Problem 1 because of the presence of the integral of the unknown solution in the asymptotic estimate (5.17). This difficulty is overcome by noting that, according to (5.17),

$$\int_0^{\infty} \Delta_*(\tau)\,d\tau = \int_0^{N} \Delta_*(\tau)\,d\tau + (\gamma-1)(1+\nu)\int_N^{\infty}\left[2\int_0^{\infty}\Delta_*(s)\,ds - \eta\right]\frac{d\tau}{\tau^3} + o(N^{-2}) \quad \text{as } N\to\infty. \tag{5.21}$$

Solving (5.21) for $\int_0^{\infty}\Delta_*(\tau)\,d\tau$ yields

$$\int_0^{\infty}\Delta_*(\tau)\,d\tau = \frac{-\frac{\eta}{2N^2}(\gamma-1)(1+\nu)+\int_0^{N}\Delta_*(\tau)\,d\tau}{1-\frac{(\gamma-1)(1+\nu)}{N^2}} + o(N^{-2}) \quad \text{as } N\to\infty. \tag{5.22}$$

In the numerical procedure, the error term $o(N^{-2})$ in (5.22) is dropped and the integral from 0 to N of Δ_* is discretized by means of the trapezoidal rule. Thus, in contrast to the situation in Problem 1, that portion of the integral in (5.1) arising from the interval $[N, N+\zeta]$ contributes to the unknowns in the system of linear algebraic equations which is ultimately obtained for the values of Δ_* at the meshpoints.

D. Results for the overlapping-filament problem. We now turn to a discussion of the numerical results for Problem 2. Figures 10 through 13 show the variation of the normalized filament force $p(z)/p(\infty)$ with distance along the filament for a fixed separation distance $\ell = 2.2a$; the overlap increases from h=0 in Figure 10 to h=20a in Figure 13. In each figure curves are shown for various values of the stiffness ratio $\gamma = E_2/E_1$, and for each stiffness ratio the corresponding curve for the single-filament case is also presented. The latter curves represent the results of Sternberg and Muki [3] and were reconfirmed by the present calculations.

No interesting effect on the load-absorption curves was obtained by varying Poisson's ratio for the matrix. All results in Figures 10 - 17 correspond to the value $\nu = 1/4$.

A comparison of Figures 10 through 13 clearly reveals the effect of progressively increasing overlap. In the first of these figures, corresponding to zero overlap, the load absorption characteristics of a filament in Problem 2 are seen to be qualitatively the same as those of a single filament. The principal quantitative difference between the two cases is the faster approach to its terminal value of the ratio $p(z)/p(\infty)$ in the overlapping-filament case.

In Figure 11 (overlap $h = 6a$) the load-absorption curves for the overlapping filaments begin to reflect some features not present in the single-filament problem, particularly at the lower stiffness ratios. The curve for $\gamma = 2$, for example, shows a relatively sudden increase in load absorption rate at a value of z/a slightly less than the dimensionless

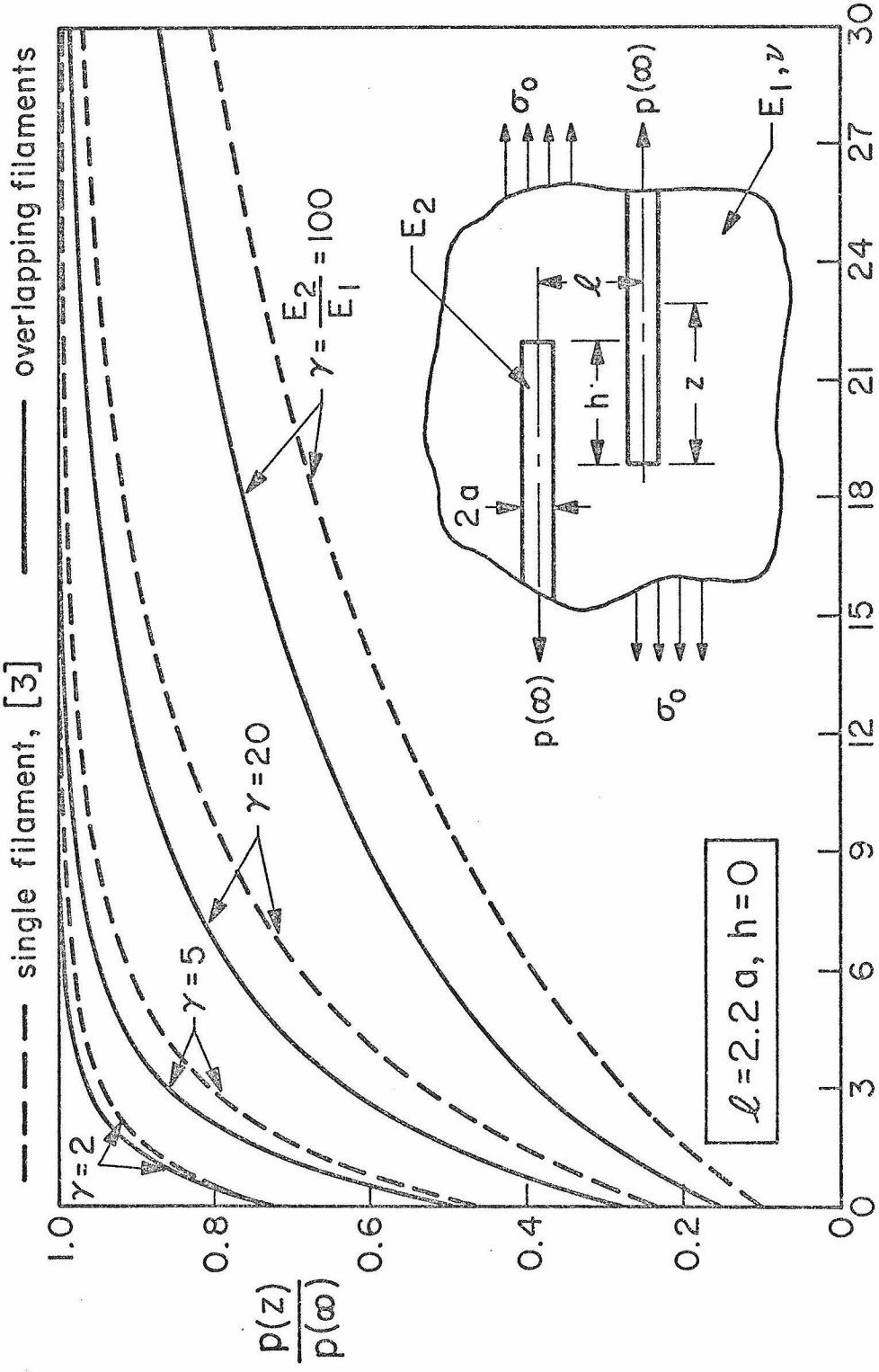

FIGURE 10. VARIATION OF FILAMENT-LOAD WITH DISTANCE ALONG FILAMENT, $\ell = 2.2a$, $h = 0$.

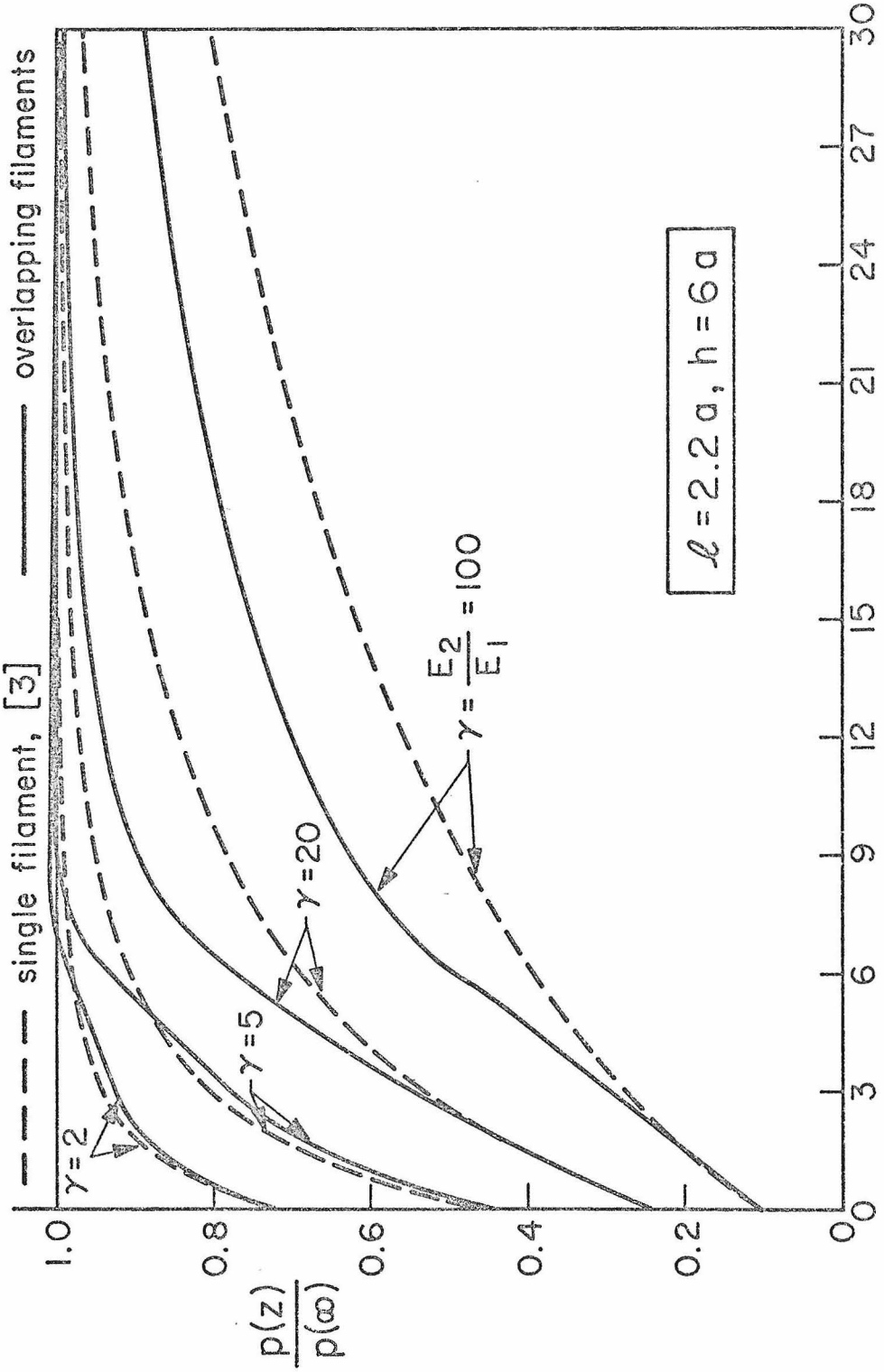

FIGURE 11. VARIATION OF FILAMENT-LOAD WITH DISTANCE ALONG FILAMENT, $\ell = 2.2\,a$, $h = 6\,a$.

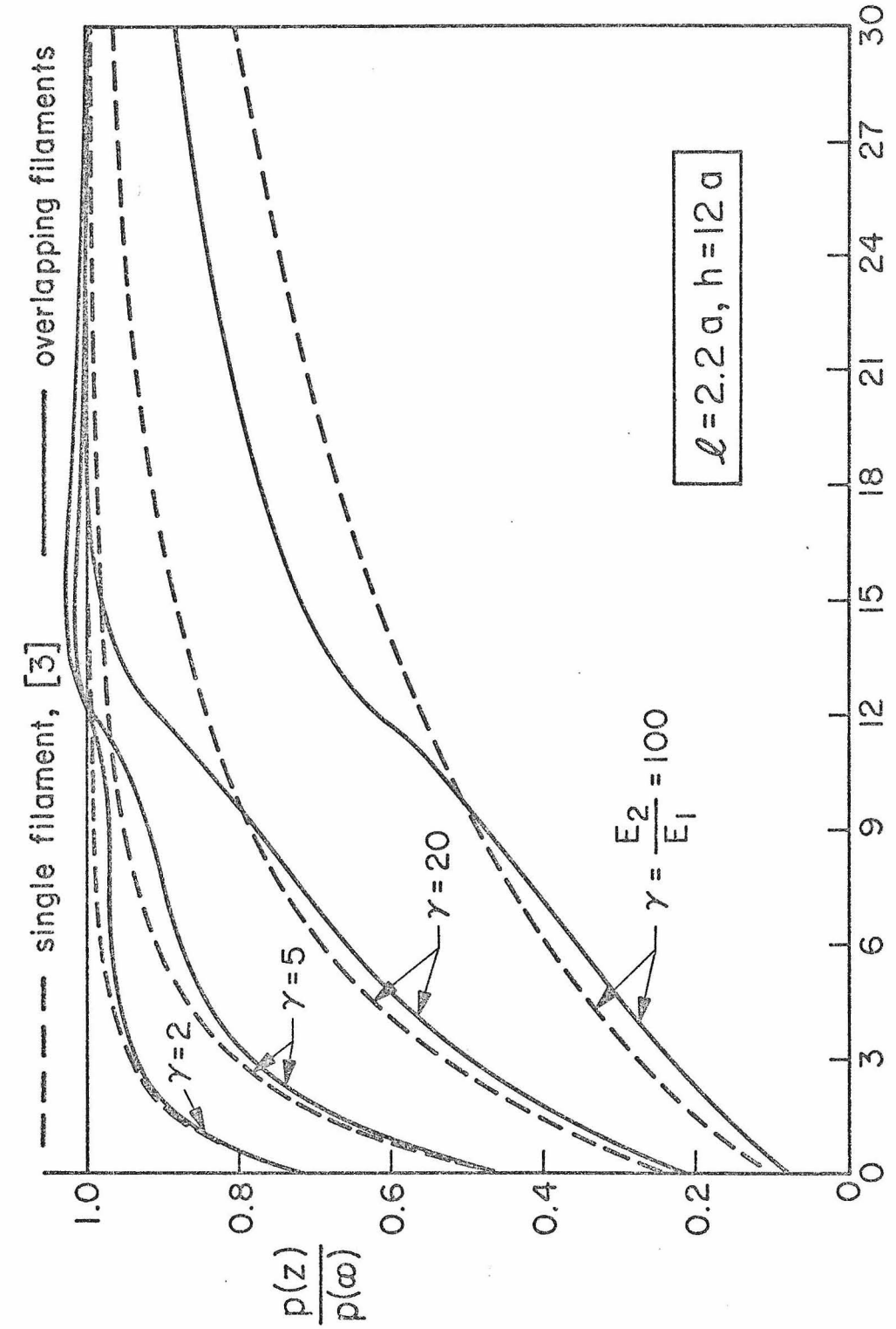

FIGURE 12. VARIATION OF FILAMENT-LOAD WITH DISTANCE ALONG FILAMENT, $\ell = 2.2\,a$, $h = 12\,a$.

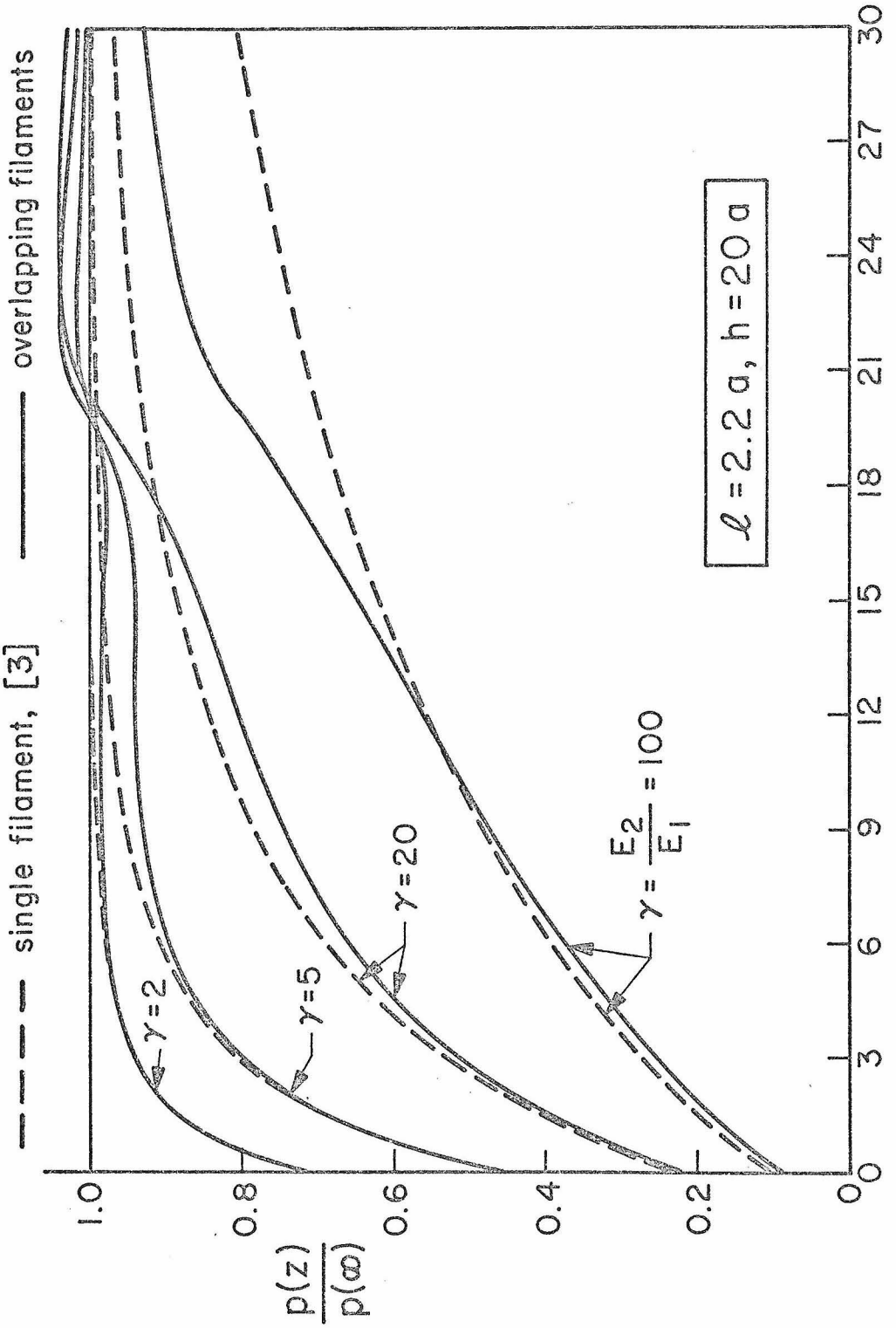

FIGURE 13. VARIATION OF FILAMENT-LOAD WITH DISTANCE ALONG FILAMENT, $\ell = 2.2\,a$, $h = 20\,a$.

overlap distance $h/a = 6$. Moreover the values of $p(z)/p(\infty)$ associated with the curves corresponding to $\gamma = 2$ and $\gamma = 5$ exceed unity over part of the range of z. This phenomenon, the possible occurrence of which was anticipated from the asymptotic analysis, becomes more pronounced, at a given stiffness ratio, as the overlap is increased to $h = 12a$ (Figure 12) and ultimately to $h = 20a$ (Figure 13). Thus the "overshoot" — in which $p(z)/p(\infty) > 1$ — appears to be increasing with increasing overlap and decreasing with increasing filament stiffness.

In order to interpret the behavior described above, we single out the overlapping-filament curve corresponding to $\gamma = 2$ in Figure 12. In one of the given filaments — let us say filament 1 — the ratio $p(z)/p(\infty)$ behaves for small z almost exactly like that for a single filament, increasing rapidly with z/a until it achieves a value of approximately 0.97, corresponding to a value of z/a of about 5. Thus filament 1 has almost "forgotten" the presence of its own end at $z = 0$ when $z/a = 5$ and, furthermore, has taken little notice up to this point of filament 2 which is only one fifth of a radius away ($\ell = 2.2a$). In Figure 12 for $\gamma = 2$, filament 1 begins to feel the effect of the end of filament 2 when $z/a = 5$ and starts to diverge from the single-filament curve. At a value of z/a of roughly 11, a further rapid increase of $p(z)/p(\infty)$ takes place, reflecting the strong local effect which the end of filament 2 exerts on filament 1. (Recall that for this curve the dimensionless overlap has the value $h/a = 12$.) One would thus expect that the behavior of the load-absorption curve under consideration for values of z/a greater than approximately 11 should be very close to that of a doubly-

infinite filament in the presence of a semi-infinite filament. One would presumably conclude that, in the presence of significant overlap, $p(z)/p(\infty)$ in a given filament always exceeds unity near the end of a neighboring filament.

Figures 14 - 17 show that the effects described above are substantially diminished when the separation between filaments is increased to $\ell = 5a$, and have virtually disappeared when $\ell = 20a$, even for an overlap of $h = 20a$.

There are some general observations which can be made from these figures. Near the end of a filament, say filament 1, an adjacent filament has little effect on the load-absorption curve of filament 1, which is very much like that of a single semi-infinite filament. On the other hand, where a nearby filament terminates, then there is a strong local effect on the load-absorption curve of filament 1. In addition, it would seem that the overlapping-filament configuration reduces the distance required for a filament to absorb a large fraction of its asymptotic load, thus decreasing its "ineffective length".

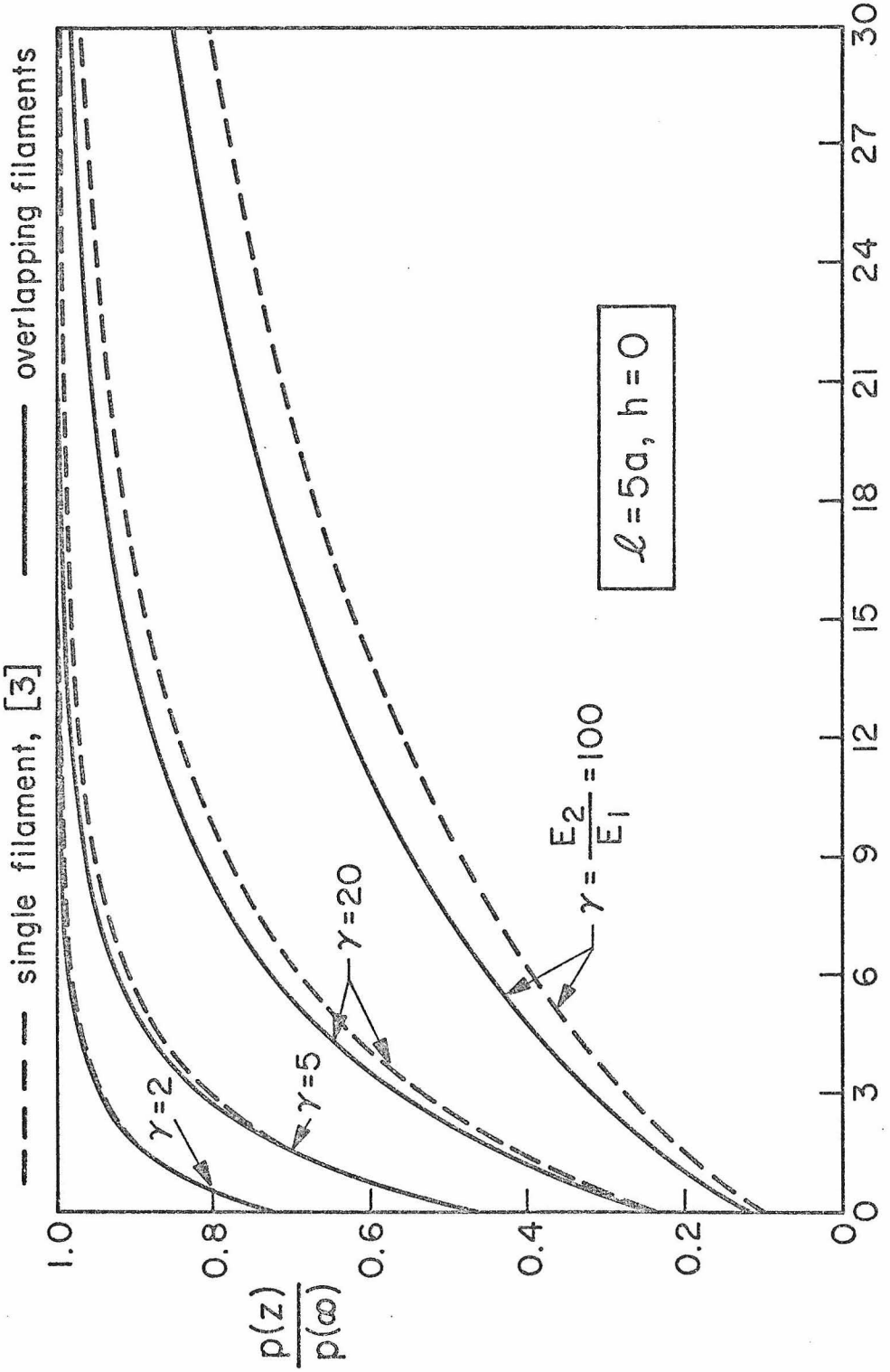

FIGURE 14. VARIATION OF FILAMENT-LOAD WITH DISTANCE ALONG FILAMENT, $\ell = 5a$, $h = 0$.

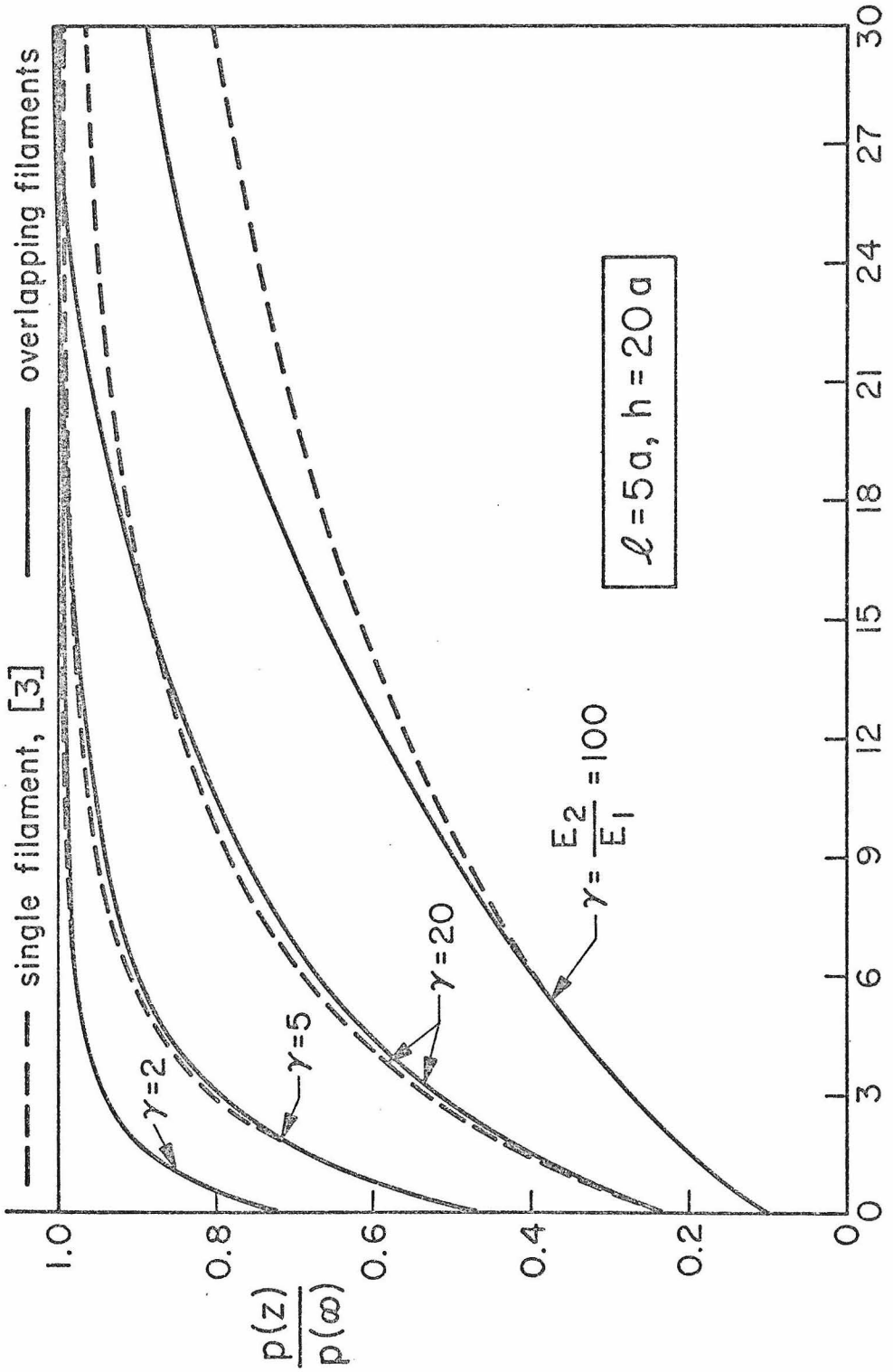

FIGURE 15. VARIATION OF FILAMENT-LOAD WITH DISTANCE ALONG FILAMENT, $\ell = 5a$, $h = 20a$.

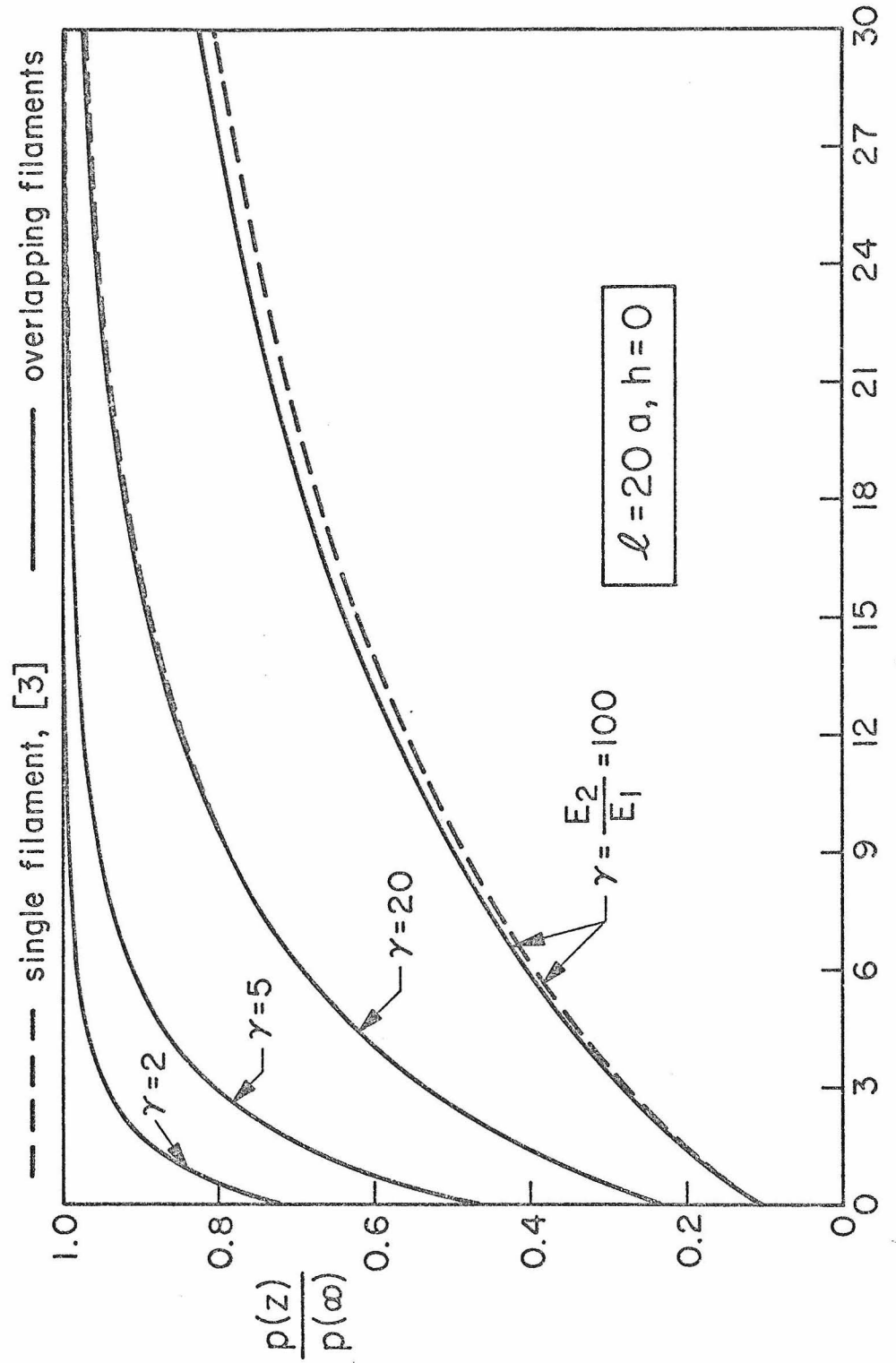

FIGURE 16. VARIATION OF FILAMENT-LOAD WITH DISTANCE ALONG FILAMENT, $\ell = 20\,a$, $h = 0$.

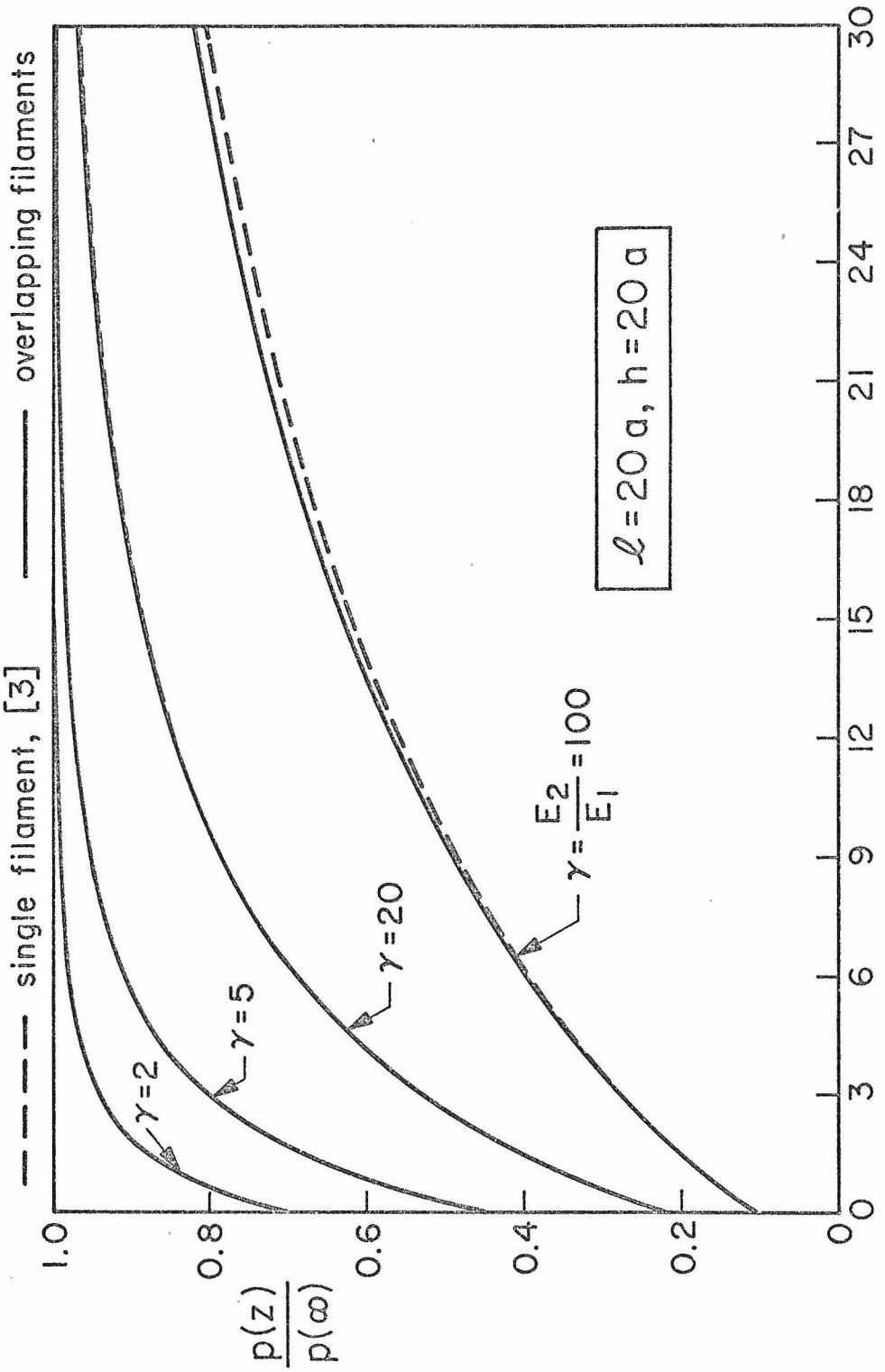

FIGURE 17. VARIATION OF FILAMENT-LOAD WITH DISTANCE ALONG FILAMENT, $\ell = 20\,a$, $h = 20\,a$.

References

[1] N. F. Dow, Study of stresses near a discontinuity in a filament-reinforced composite metal, Technical Information Series, Report R63SD61, General Electric Company (1963).

[2] B. W. Rosen, Mechanics of composite strengthening, Chapter 3 in Fiber Composite Materials, American Society for Metals (1965).

[3] E. Sternberg and R. Muki, Load-absorption by a filament in a fiber-reinforced material, Zeitschrift für angewandte Mathematik und Physik, 21/4, p. 552 (1970).

[4] R. Muki and E. Sternberg, On the diffusion of an axial load from an infinite cylindrical bar embedded in an elastic medium, International Journal of Solids and Structures, 5/6, p. 587 (1969).

[5] L. J. Cohen and J. P. Romualdi, Stress, strain and displacement fields in a composite material reinforced with discontinuous fibers, Journal of the Franklin Institute, 284/6, p. 388 (1967).

[6] P. E. Chen, Strength properties of discontinuous fiber composites, Polymer Engineering and Science, 11/4, p. 51 (1971).

[7] A. E. H. Love, A treatise on the mathematical theory of elasticity, Fourth Edition, Dover, New York, 1944.

[8] R. Muki and E. Sternberg, Elastostatic load-transfer to a half-space from a partially embedded axially loaded rod, International Journal of Solids and Structures, 6/1, p. 69 (1970).

[9] G. N. Watson, A treatise on the theory of Bessel functions, Second Edition, Cambridge University Press, 1962.

[10] H. Weber, Über die Besselschen Funktionen und ihre Anwendungen auf die Theorie der elektrischen Ströme, J. reine angew. Math., LXXX, 75 (1873).

[11] G. Eason, B. Noble and I. N. Sneddon, On certain integrals of Lipschitz-Hankel type involving products of Bessel functions, Philosophical Transactions of the Royal Society of London, Series A, 247, p. 529 (1955).

[12] Bateman Manuscript Project, Table of integral transforms, vol. 1, McGraw-Hill, New York, 1954.

[13] R. Muki and E. Sternberg, Note on an asymptotic property of solutions to a class of Fredholm integral equations, Quarterly of Applied Mathematics, 28/2, p. 277 (1970).